FEDERAL UNIVERSITY OF SANTA CATARINA
JOINVILLE TECHNOLOGICAL CENTER
AUTOMOTIVE ENGINEERING

LEONARDO NOGUEIRA CALDAS

DEVELOPMENT OF TEST BENCH FOR MOTORCYCLE HANDLEBAR VIBRATION ANALYSIS AND VALIDATION THROUGH MULTIPLE PARTICLE DAMPER

Joinville
2024

LEONARDO NOGUEIRA CALDAS

DEVELOPMENT OF TEST BENCH FOR MOTORCYCLE HANDLEBAR VIBRATION ANALYSIS AND VALIDATION THROUGH MULTIPLE PARTICLE DAMPER

Graduation Thesis submitted to the Automotive Engineering Undergraduate Program of Federal University of Santa Catarina to obtain the title of Bachelor in Automotive Engineering.

Advisor: Prof. Thiago Antonio Fiorentin, Dr.

Co-Advisor: Prof. Andrea Piga Carboni, Dr.

Joinville
2024

LEONARDO NOGUEIRA CALDAS

DEVELOPMENT OF TEST BENCH FOR MOTORCYCLE HANDLEBAR VIBRATION ANALYSIS AND VALIDATION THROUGH MULTIPLE PARTICLE DAMPER

Graduation Thesis submitted to the Automotive Engineering Undergraduate Program of Federal University of Santa Catarina to obtain the title of Bachelor in Automotive Engineering.

Joinville (SC), June 24, 2024.

Examining Board:

Prof. Thiago Antonio Fiorentin, Dr.
Advisor/Committee President
UFSC

Prof. Andrea Piga Carboni, Dr.
Evaluator
UFSC

Prof. Antônio Otaviano Dourado, Dr.
Evaluator
UFSC

Prof. Marcos Alves Rabelo, Dr.
Evaluator
UFSC

ACKNOWLEDGEMENTS

First and foremost I wish to thank my one and only Tay for putting up with all the stressful days and craziness during some periods in the making of this work. Also, I would like to thank my parents Maria Rita and Antonio Carlos for being the most loving family I could have, you provided me with more than I ever hoped for in every step of my life. Thank you all for guiding, supporting and encouraging me along every step I have taken.

I would like to thank my professors Thiago Antonio Fiorentin and Andrea Piga Carboni for the unconditional support through out this work. I really appreciate your enthusiasm and will for pursuing new research topics, and mostly your passion for making projects become a reality. I am very grateful for the opportunity you gave me, thank you very much!

I wish to thank the friends I have made along this journey called UFSC. I won't go into names at the risk of forgetting someone, because there is too many good people in this university. At the beginning most of them were part of our local Formula SAE student team but this number has grown over the years. Thank you guys from LAV and LASUB for always helping me without asking anything in return. I would also like to acknowledge the support professors Sérgio Junichi Idehara and Thiago Pontin Tancredi for the great advice and for being such caring persons.

Finally, I wish to extend my gratitude to the Santa Catarina Foundation for Education and Research (FESC) for providing the highest quality equipment, as well as, financial support that enabled this work.

RESUMO

Vibrações induzidas por motocicletas têm sido esparsamente estudadas nos últimos 20 anos. Até agora, já se reconheceu o impacto dessas vibrações nos motociclistas, mas não foram tomadas medidas suficientes para reduzir as doenças musculoesqueléticas que os motociclistas regulares estão destinados a sofrer. Para abordar esse problema, as vibrações mão-braço devem ser cuidadosamente estudadas. Caracterizar o comportamento dinâmico de estruturas complexas não é uma tarefa trivial, e torna-se ainda mais desafiador com a inclusão de absorvedores não lineares, como amortecedores de múltiplas partículas. Portanto, fornecer um ambiente de teste confiável que abstraia alguns dos desafios é fundamental para otimizar o desenvolvimento de novos absorvedores de vibração. Este trabalho tem como objetivo delinear tanto o *hardware* quanto o *software* para futuras pesquisas sobre esse tema. Várias configurações de bancadas de teste foram testadas e comparadas entre si. Por fim, foram conduzidos experimentos com o intuito de validar o sistema de aquisiçao de dados através da verificação dos efeitos do material das partículas e da taxa de preenchimento da carcaça na eficiência geral de um amortecedor de múltiplas partículas.

Palavras-chave: Controle de Vibrações. Vibrações em Motocicletas. Bancada de Testes. Amortecedores de Multiplas Particulas.

ABSTRACT

Motorcycle induced vibration's have been sparsely studied over the last 20 years. So far it's burden on the riders have already been acknowledged. but not enough measures were taken to reduce the musculoskeletal diseases regular riders are fated to suffer from. By means of tackling this issue, hand-arm vibrations must be thoughtfully studied. Characterizing the dynamic behavior of complex structures is not a trivial task. Which is pushed even further with the inclusion of non-linear absorbers such as multiple particle dampers. Therefore, providing a reliable test environment that abstracts some of the challenges is critical for optimizing the development of new vibration absorbers. This work is intended to layout the hardware and software for future researches along this topic. Several test bench configurations were tested and compared against each other. Finally, experiments were conducted to validate the data acquisition system by examining the effects of particle material and filling rate on the overall efficiency of a multiple particle damper.

Keywords: Vibration Control. Motorcycle Vibration. Test Bench. Multiple Particle Damper.

LIST OF FIGURES

LIST OF TABLES

LIST OF ACRONYMS

AC Alternate Current

ADC Analog to Digital Converter

DAC Digital to Analog Converter

DAQ Data Acquisition

DAS Data Acquisition System

DC Direct Current

DFT Discrete Fourier Transform

DOF Degrees of Freedom

DUT Device Under Testing

DVE Daily Vibration Exposure

EAV Daily Exposure Action Value

ELV Daily Exposure Limit Value

EMA Experimental Modal Analysis

FEM Finite Element Method

FFT Fast Fourier Transform

FRF Frequency Response Function

HAV Hand-Arm Vibrations

HAVS Hand-Arm Vibration Syndromes

IEPE Integrated Electronics Piezo-Electric

I/O Input/Output

LabVIEW Laboratory Virtual Instrument Engineering Workbench

LPF Low-Pass Filter

MPD Multiple Particle Damper

MPE Modal Parameter Estimation

MSDs Musculoskeletal Disorders

NI National Instruments

ODS Operational Deflection Shape

PSD Power Spectral Density

RMS Root Mean Square

RPM Revolutions per Minute

SMPS Switched-Mode Power Supply

TMD Tuned Mass Damper

UI User Interface

VI Virtual Instrument

VWF Vibration Induced White Finger

VTV Vibration Total Value

WBV Whole Body Vibration

WMSDs Work-Related Musculoskeletal Disorders

USB Universal Serial Bus

CONTENTS

1 INTRODUCTION

Over the last 20 years, motorcycles have consolidated their role as a means of transportation, while in South Asian countries, they represent at least 60% of the fleet. In contemporary times, two-wheeled electrical vehicles such as scooters, e-bikes and electric motorcycles, presented themselves as a tangible opportunity for those who used public transportation daily; thus contributing even further to the growing number of users (RAJPER; ALBRECHT, 2020).

Despite the growth in the sector, regulations are not keeping pace with the industry, resulting on a lack of guidance regarding health and safety issues. A number of studies have reported on this mater, finding that workers are fated to develop Work-Related Musculoskeletal Disorders (WMSDs) when riding a motorcycle for more than five hours per day (MIRBOD et al., 1997; DIYANA et al., 2019).

Ride comfort is deeply associated with the vibration levels, as well as, the frequency bands that compose the excitation to which the rider is subjected. Since the natural frequencies of the human body range from 1 up to 50 Hz, this interval must be addressed during the vehicle's development phase, otherwise the resulting product will induce sickness and in extreme cases might be unbearable to ride (GRIFFIN, 1990).

Although frequencies above 50 Hz may be less severe to the human body, their presence along the ride can build up to undesirable side effects. Literature findings indicate that rider discomfort precedes the manifestation of Musculoskeletal Disorders (MSDs) and is a causal factor in motorcycle accidents, since it directly disturbs the cognitive capacity (ARUNACHALAM et al., 2018).

The specific causes of MSDs have not yet been determined; however, the analyzed papers agree on the detrimental impact of Hand-Arm Vibrations (HAV). In between the variables that impose difficulty on the characterization of the sources of MSDs are different riding conditions, rider stress levels, risks embedded with real-world experiments, instrumentation procedures, equipment utilized during experiments and finally the lack of follow up on existing research (OSPINA; JIMÉNEZ, 2019).

Existing literature on motorcycle testing methodologies share common objectives, provide a safe and controllable environment, that may be used for studies regarding the definition of subjective comfort parameters, riders' vibration exposure measurements, vibration absorbers development and motorcycle dynamics. Those objectives have lead to the development of test benches with distinct characteristics that are embedded in one of the following configurations: isolated handlebars, partial motorcycle systems and also complete motorcycles.

Amidst the current vibration suppression techniques, the passive absorbers and lately the active absorbers have been extensively studied over several applications. Regarding motorcycle-focused research, only a handful of researchers have published on this matter. As a consequence, not only publications on this mater are sparse, but also the discussions are carried over very specific scenarios, posing a challenge for continuing the line of research in a comprehensive manner.

Considering the arguments presented, it is proposed to engineer a test bench that is able to stimulate a generic, single piece, motorcycle handlebar. Along with the mechanical components a software tool shall be developed through a LabVIEW Application with intent of enabling the generation deterministic and random signals, as well as acquisition, processing and visualization of acceleration signals.

1.1 OBJECTIVES

1.1.1 Main Objective

Develop a test bench capable of generating vibrations that represent ordinary motorcycle use on public roads, in such way that the handlebar excited by the test bench show modal forms analogue to a real world equivalent situation. Subsequently, use this apparatus to verify the efficiency of multiple particle dampers.

1.1.2 Specific Objectives

- Identify vibration modes of a motorcycle handlebar under real real world operation;
- Implement a Data Acquisition Software capable of acquiring and generating signals;
- Demonstrate the efficiency of the excitation source through the output of harmonic and pseudo-random signals;
- Validate the Data Acquisition System solution through comparison with professional and calibrated equipment;
- Verify the efficiency of passive dampers under random excitation;

2 THEORETICAL FOUNDATION

In the context of engineering a vibration test bench, with the goal of validating vibration absorbers, this chapter addresses critical areas of study to achieve the proposed objectives. It provides an overview of handlebar vibrations, including their influence over the rider's health, as well as sources of vibration and generic handlebar mode shapes. The chapter also looks into vibration suppression using passive absorbers, with a specific focus on multiple particle dampers. Finally, this chapter introduces the fundamental concepts of vibration analysis and instrumentation, and includes a short review of state-of-the-art research.

2.1 HANDLEBAR VIBRATION

The human response to vibration can be classified as Whole Body Vibration (WBV) or HAVs, these classifications differ on the path described from the source of the vibration through the human body. While riding a motorcycle, there are three main contact points between the human body and the vehicle: the handlebars, the foot rests and the seat, in this way, a motorcycle rider is subjected to both WBV and HAV.

Field experiments point out that the most affected areas due to the exposure to motorcycle vibrations are neck and shoulders (MIRBOD et al., 1997; DIYANA et al., 2019). This is corroborated by the literature, which indicates that the magnitude of the accelerations on motorcycle handlebars often exceeds the Daily Vibration Exposure (DVE) recommended by the European Directive 2002/44/EC (NOH et al., 2017; JELACIC; PIKULA, 2019).

Åström et al. (2006) suggested that there is a correlation between HAV magnitude and the grip force applied by the rider; thus, higher vibration magnitude might increase the impedance between the handlebar and hands, resulting in a greater load upon the upper limbs. This, in turn, can lead to discomfort which precedes the emergence of MSDs. These findings reiterates the endeavor of characterizing HAV, under the high number of variables involved on the measurement process, as well as, the importance of developing less complex environments for vibration studies.

Motorcycle-focused academic literature has been concentrated on diagnosing the causes and the consequences of Hand-Arm Vibration Syndromes (HAVS) with the aim of improving comfort and safety of two-wheeled vehicles. So far, the topics covered by research can be categorized as the development of vibration suppression devices, causes of MSDs, causes WMSDs, general topics regarding the consequences of the discomfort caused by vibrations, as well as topics beyond the scope of this work (CHEN et al., 2009; CHELI et al., 2011; RASHID et al., 2021).

In accordance with Griffin (1990), there are four recurrent types of HAVS, namely vascular disorders, bone and joint disorders, peripheral neurological disorders and muscle disorders. Among motorcyclists, HAVS manifest mostly as Vibration Induced White Finger (VWF), lower back and shoulder pain (MIRBOD et al., 1997; CHEN et al., 2009). Not only do they pose a public health issue, Yousif et al. (2020) concluded that the discomfort might compromise the rider's attention and contribute to the ever-increasing number of traffic-related fatalities.

In sight of addressing the public health issue presented by WMSDs, in 2002, the European Parliament sanctioned the directive 2002/44/EC. The document outlines employer obligations, along with threshold levels of DVE for both HAV and WBV accounted for a eight hour period. The Daily Exposure Action Value (EAV) is a boundary from which actions should be taken and the Daily Exposure Limit Value (ELV) stands for a maximum allowed limit (Table 1) (EUROPEAN PARLIAMENT, 2002).

Table 1 – Exposure limit values and action values deliberated by European parliament

Exposure Value	Affected Areas	Limit Value m/s^2
EAV	HAV	2.5
	WBV	0.5
ELV	HAV	5
	WBV	1.15

Source: (EUROPEAN PARLIAMENT, 2002)

The foundation for the aforementioned directive resides on the standards (ISO, 2001a) and (ISO, 2001b), which are practical guides for measurement and evaluation of HAV. The standard provides the calculations for the (Vibration Total Value (VTV)), (Equation 1) and the DVE (Equation 2), as well as insights into the appropriate frequency weighting and band filters (Figure 1) that should be applied to the acquired data.

$$a_{hl} = \sqrt{(k_x \cdot a_{hwx})^2 + (k_y \cdot a_{hwy})^2 + (k_z \cdot a_{hwz})^2} \tag{1}$$

$$A(8) = \sqrt{\frac{1}{T_0} \sum {a_{hv_i}}^2 T_i} \tag{2}$$

Figure 1 – Hand-Arm (Wh) Vibration Weighting Curve from ISO 5349-1.

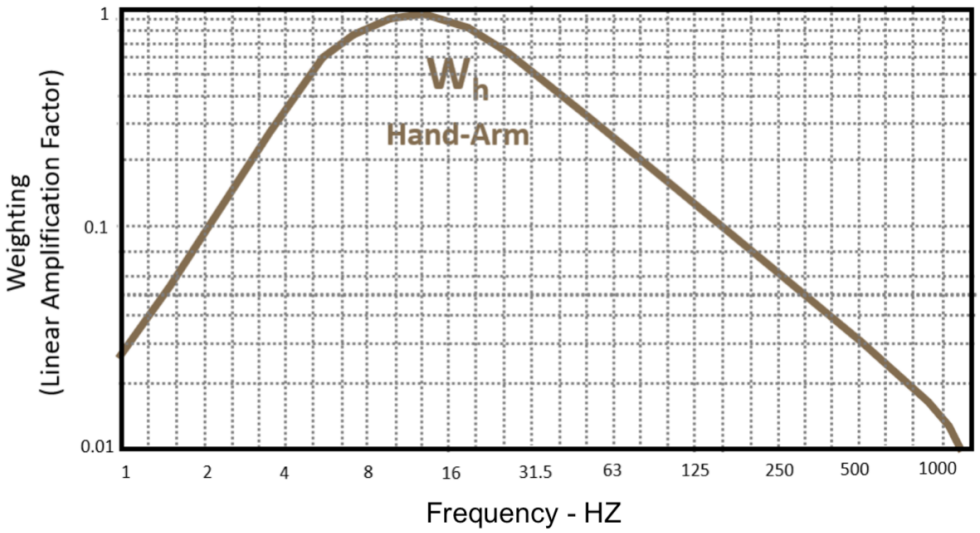

Source: Schaldenbrand (2021)

2.1.1 Sources of Hand-Arm Vibrations

Previous studies have reported that the vibration exposure level to which the rider is subjected is a function of road conditions, vehicle dynamic characteristics, vehicle maintenance, engine configuration and on driver's characteristics such as age, experience, sitting posture and body weight (CHEN et al., 2009). Therefore, HAV is not solely determined by the road conditions and the motorcycle characteristics but also by the rider's interaction with the motorcycle.

Nevertheless, handlebar vibrations originate mostly from the unevenness of the road and from inertial imbalances caused by combustion engines. As per Falco et al. (2013), these are the only sources within a frequency range that might induce a resonance condition. Yokomori et al. (1986) also found that, regardless of the road conditions - whether asphalt, gravel or snow - the handlebar vibrations were always in sync with the engine's RPM for the motorcycle under testing. Figure 2 provides a graphical representation of the limited relevance of the motorcycle speed in spite of the maximum vertical acceleration recorded. This behavior is corroborated by Usamah et al. (2022) measurements that correlate the acceleration magnitude with engine speed (Figure 3).

Figure 2 – RMS acceleration in the vertical direction on a paved surface.

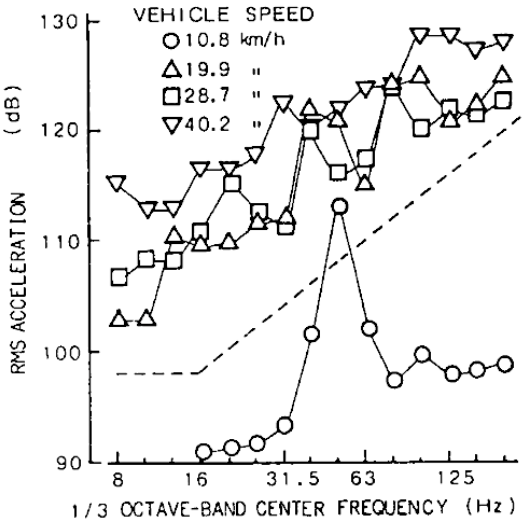

Source: Yokomori et al. (1986).

Hence, as Fasana and Giorcelli (2010) noted, handlebar accelerations occur between 50 Hz and 300 Hz, primarily in the vertical direction. Within this specified range, a resonance condition is likely to occur on the handlebars, given their natural frequency revolves around 100 Hz. Falco et al. (2013) findings reiterates the influence of the frequencies generated by combustion engines, by performing a modal analysis at constant RPM, which can be observed at figure 4, where F_{no} and F_{nv} stands for the horizontal and vertical natural frequencies respectively.

Figure 3 – Handlebar vertical acceleration measurements as a function of engine speed.

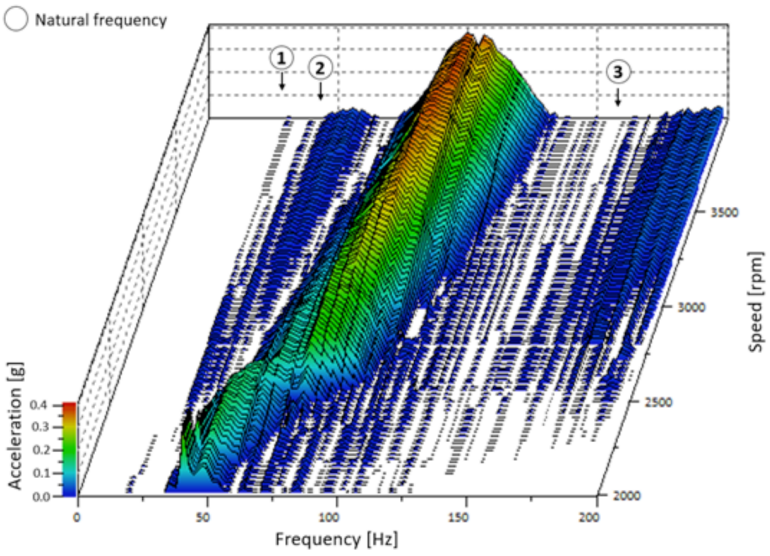

Source: Usamah et al. (2022).

Figure 4 – Handlebar acceleration for static motorcycle with engine running at 4800 RPM.

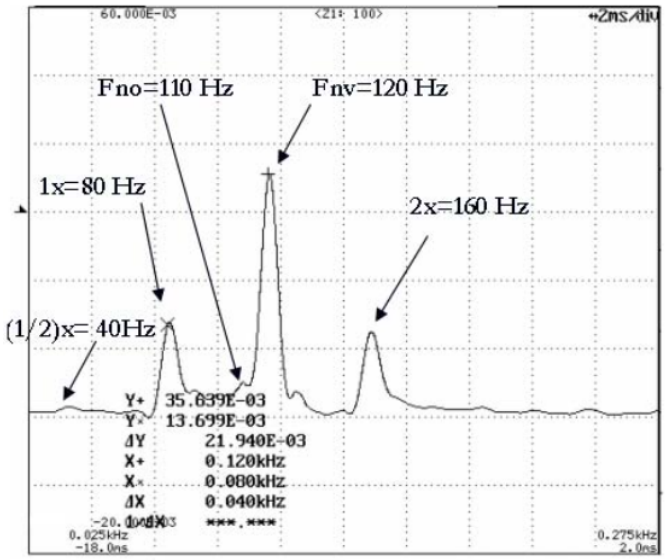

Source: Falco et al. (2013).

According to Cossalter (2006), there are three major modes of vibration associated to motorcycles the capsize, weave and wobble. Even though wobble is characterized as an oscillation of the front end, which is coupled directly to the handlebar, it's frequency ranges from 5 Hz until 10 Hz. Since this bandwidth is significantly lower than the handlebar resonance frequency and the output torque is applied along the steering axis, it should be addressed as a safety issue as it unbalances the motorcycle.

As for capsize and weave, these modes also have minimal impact on tactile vibration comfort. Capsize is a non-oscillating mode and, therefore, can be dismissed from the HAV standpoint. Weave is defined as an oscillation of the entire motorcycle, with frequencies ranging from 0 up to 4 Hz. Given that this frequency range is substantially lower than the handlebar's resonance frequency, weave, like wobble, does not significantly contribute to comfort related tactile vibrations.

Moreover, as Falco et al. (2013) concluded, the low resonance frequency of wheel unbalances excludes them as significant contributors to high-magnitude vibrations on the handlebars. This is attributed to the natural frequency of handlebar components surpassing that of wheel unbalances by more than one order of magnitude, dismissing their relevance to this study. These insights collectively guide the focus toward a refined examination of specific directional sources, such as the vibrations caused by the engine unbalances, which holds greater significance in understanding the dynamics of handlebar vibrations that affect the ride comfort.

2.1.2 Natural Frequencies and Mode Shapes

Mode shapes describe mathematically the spatial distribution or vibration pattern that a system exhibits when excited to its natural frequencies. For systems with well-defined models, modal parameters — natural frequencies, mode shapes, and damping factors — can be calculated by solving the equations of motion (INMAN, 2014). However, this is not the case for most structures. Therefore, modal parameters are usually calculated based on Frequency Response Function (FRF) obtained via experimental testing or simulation methods such as the Finite Element Method (FEM).

Despite the varying conditions and research objectives in the literature on handlebar vibrations, the data provided offers valuable insights. The natural frequencies reported in the reviewed studies are summarized in Table 2 where each column contains resonance frequencies documented. This table serves as a comprehensive guide to understanding the range of frequencies observed in different contexts. The discrepancies between the reported values can be attributed to differences in materials and geometries, which directly influence the mass, stiffness, and damping of the structure. Additionally, fixtures affect the dynamic behavior of the structure. To better understand these influences, it is important to address several key concepts in modal analysis, including the nodes of a mode shape and rigid-body modes.

Table 2 – Handlebar's natural frequencies obtained through EMA under different constraints.

Mode	Frequency[Hz]							
	Motorcycle				Rigid Structure		Free-Free Condition	
1	33	41.6	91	91.9	190	46.05	114.9	60
2	71	82.2	94	94.87	578	56.11	299.9	297
3	232	183.0	110	99.8		64.54		
4			112.5	421		156.7		
5				472				

Source: Author (2023).

A node of a mode is defined as a coordinate where the respective mode shape element is zero, indicating no displacement at that point. For instance, in practical experiments, sensors should never be placed at these nodes, as no response will be measured. Rigid-body modes, on the other hand, are associated with unrestrained structures and may exhibit vibration modes not related to deflection, but rather to the overall movement of the structure around its equilibrium point. Given the focus of this research on local modes, which concentrate most of the vibrations within a subsystem, rigid modes should be identified and discarded from further analysis (INMAN, 2014).

Ro et al. (2007) analysed a carbon-fiber handlebar in depth both experimentally and through FEM simulation. The EMA was performed with an impact hammer

and the displacement was measured with a contactless laser sensor. The results indicate the presence of two natural frequencies in between 33 and 578 Hz, and the associated mode shapes are depicted in figure 5. The first mode at 190 Hz corresponds to a rigid body mode, where the handlebar twists it self around the fixture in the center. As for the second mode at 578 Hz, it is visible that there are two points with acceleration tending to zero which are called nodes of a shape.

Figure 5 – Carbon-fiber handlebar mode shapes.

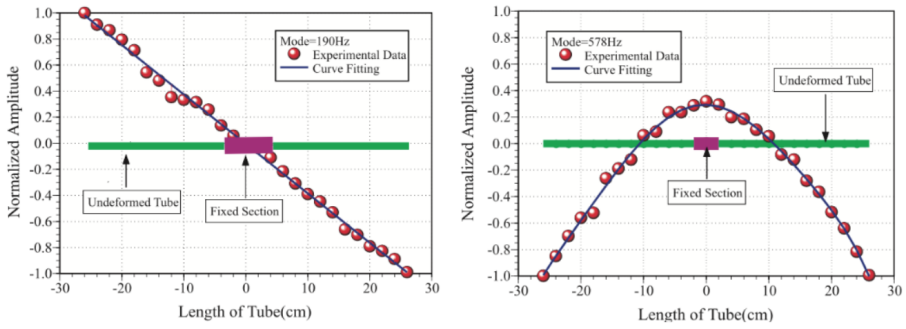

(a) (b)

Source: Adapted from Ro et al. (2007).

Setia et al. (2019) also performed an impact test, although the handlebar was instrumented with an Integrated Electronics Piezo-Electric (IEPE) accelerometer. In this study, the handlebar was suspended by a flexible cable attached to its center as shown in figure 6. This experiment configuration is often referred to as Free-Free Modal Analysis. Given the unrestrained condition, the resulting FRF contained rigid-body modes along with the modes of interest found at 114.9 Hz and 299.9 Hz.

Figure 6 – EMA setup and results.

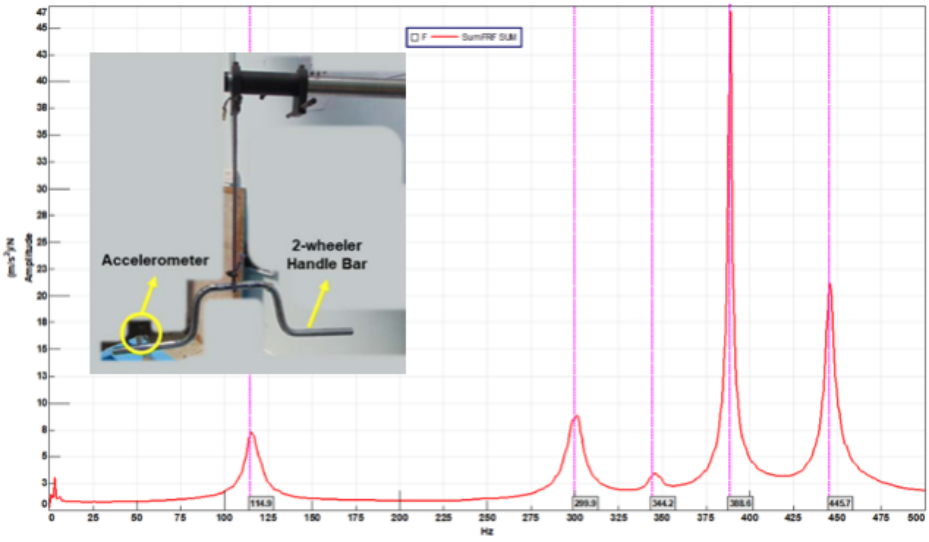

Source: Adapted from Setia et al. (2019).

In contrast, Usamah et al. (2022) conducted the EMA with the handlebar attached to the motorcycle. Trials were performed both with and without a rider gripping the handlebar, as shown in figure 7. From these experiments, the relevant natural frequencies were defined as 41.6 Hz, 82.2 Hz, and 183.0 Hz.

Figure 7 – Horizontal and vertical FRFs of a handlebar excited by an impact hammer.

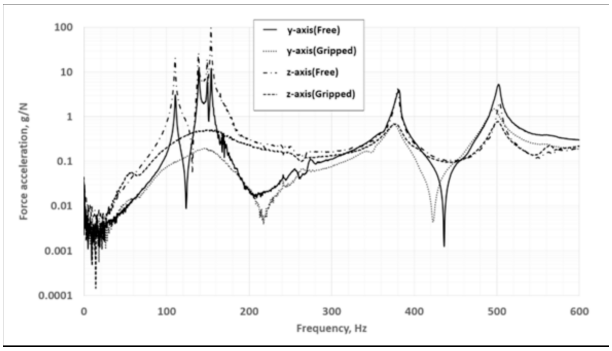

Source: Usamah et al. (2022).

Even though the experiments were conducted with different handlebars and fixtures, the documented results are comparable to each other. Along this line, it is plausible to conclude that the first six vibration modes of a generic handlebar should be contained from 30 Hz to 500 Hz.

2.2 VIBRATION SUPPRESSION

The field of vibration suppression has been extensively studied from various perspectives; thus far, Yang et al. (2022) compiled the tuned mass dampers (TDMs) systems and their configurations over the last 30 years, Richiedei et al. (2022) discussed dynamic structural modification as a vibration suppression method, Ehlers et al. (2020) proposed a particle damper solution that is embedded on the beam structures manufactured by laser powder bed fusion (LPBF) and further on designed a motorcycle triple clamp aiming for a light-weight, high-rigidity and high-damping final component (EHLERS; LACHMAYER, 2020).

As with any engineering problem, designing vibration suppression devices for motorcycles involves navigating trade-offs and making compromises. Motorcycle suspensions, for instance, are meticulously engineered to fulfill various objectives, including maintaining tire-road contact, managing motorcycle trim, and enhancing rider comfort. Amidst these multifaceted demands, higher frequency vibrations, typically above 20 Hz, often receive less attention and may be overlooked in traditional suspension designs. Therefore, dedicated devices are required to address these higher frequency vibrations.

While higher quality production motorcycles may already feature some vibration suppression mechanisms, such as counterweights, tuned mass dampers, and more recently, active vibration dampers, there remains a need for solutions capable of effectively mitigating vibrations that may induce discomfort. These solutions, which leverage Artificial Intelligence and Machine Learning for terrain prediction and adaptive ride adjustments, represent promising avenues for enhancing motorcycle ride quality and safety.

Although theoretically there is great diversity off methods, real world implementations of vibration absorbers are limited by production liabilities namely manufacturability and budget, as well as, physical constraints related to size and mass. For this reason, even the well known tuned mass dampers (TMDs) are restricted to higher grade production motorcycles and after-market components, while the positioning of mass on strategic positions is presented as the most popular strategy for managing the dynamic behavior of a motorcycle handlebar.

2.2.1 Tuned Mass Dampers

Tuned mass dampers or even tuned vibration absorbers, are devices designed to eradicate the displacement of a component under a harmonic excitation, by means of matching the disturbance force with equal magnitude and opposite direction. On it's simplest configuration, the TMD is doomed to achieve the expected performance only at the frequency it has been tuned for, therefore more robust configurations have been envisioned and are presented at figure 8.

Figure 8 – Popular TMD system's configurations.

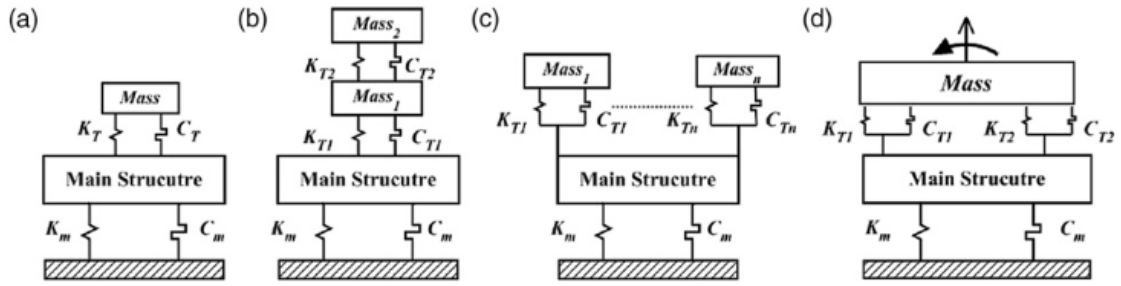

Source: Yang et al. (2022).

Due to it's narrow efficiency range, TMDs require tight manufacturing tolerances otherwise the resulting product might be tuned for the wrong frequency, leading to a loss of efficiency. Under extreme circumstances, this misalignment may exacerbate vibrations further. Moreover, the effective range of the TMD to the optimal frequency can be increased by the use of dampers, at the cost of not achieving zero displacement (INMAN, 2014).

The reported research on TMD with intent of reducing HAV mostly aimed at higher capacity motorcycles that have segmented handlebars instead of the traditional single tube ones. Fasana and Giorcelli (2010) and Agostoni et al. (2012) have developed prototypes with proven efficiency for a specific resonance frequency assumed to be the one that causes greater discomfort. Both prototypes rely in the exploitation off a concentrated mass placed at both extremities of the handlebar. The referred mass original intent was the improvement of vehicle stability by controlling the Wobble mode described in section 2.1.2. The results obtained display the original response of the handlebar against the responses with additional mass in the extremity of the handlebar, incorrectly tuned TMD and tuned TMD (Figure 9).

Figure 9 – Experimental response of the handle with and without the absorber.

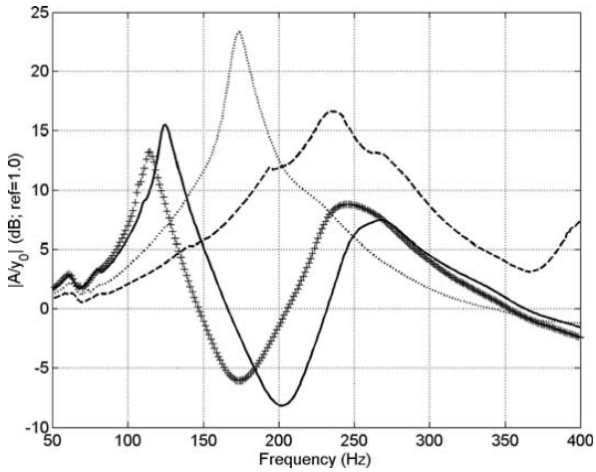

Source: Fasana and Giorcelli (2010).

2.2.2 Multiple Particle Dampers

Particle dampers (PDs) or granular dampers are a vibration suppression method which absorbs kinetic energy due to the inelastic collision of particles contained in a enclosure, the absorbed energy is then converted to thermal and acoustic energy. As opposed to the TMDs, Multiple Particle Dampers (MPDs) are a strictly nonlinear and therefore do not have analytical solutions based on their movement equation, hence, it is crucial to conduct experimental studies along with the development process.

In contrast with modeling complexity, MPDs are suitable for several applications due to it's mechanical simplicity, low demand for maintenance, ease of manufacture and capability of withstanding severe conditions. Additionally, according to Lu et al. (2018), when properly tuned these vibration absorbers are capable of mitigating vibrations over a broader frequency range when compared to the TMDs limited effective interval.

The vibration absorption is a consequence of the collision and friction between particles and between particles and the enclosure (Figure 10), both scenarios result in momentum exchange and energy dissipation through several mechanisms, in particular heat and noise. As a result, their performance is a function of the particle's material properties, as well as it's size, shape, quantity and mass. Moreover the enclosure characteristics such as geometry, wall thickness and material are also variables to be accounted for (PRASAD et al., 2022).

Figure 10 – Schematic diagram of a passive MPD.

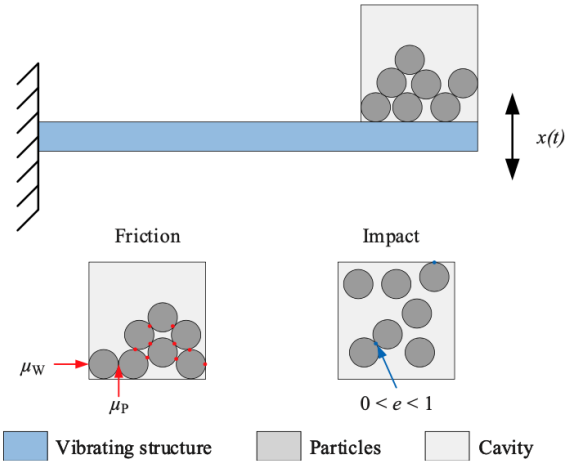

Source: (EHLERS et al., 2020).

Ehlers et al. (2020) performed an experimental analysis to ascertain the damping ratio (D) of a laser-melted test specimen constructed of AlSi10Mg. The obtained results confirm that as long as the excitation source and material were consistent with those used in the experiment, modal parameters might be estimated for similar structures. Several authors describe simplified models that estimate modal parameters based on curve fitting of experimental data points. Although these methods are straightforward and yield good results under a set of restrictions, they produce models that are coupled to the characteristics of the input data.

Alternative models that disregard inter-particle interactions can offer broader representativity and may decrease the number of prototypes that need to be tested and validated, which in turn reduce development costs. Lu et al. (2020) proposed a particle model where the resulting system can be conceptualized as a particle interacting with its enclosure through two springs and two dampers (Figure 11), simulating collisions with the enclosure walls. In this setup, the spring component (k_p) represents the kinetic energy, accounting for friction within its calculation, while the viscous damper (c_p) serves to encompass the energy dissipation mechanisms associated with the collisions. Additionally, the coupling between the absorber and the structure is represented by yet another spring (k) and viscous damper (c).

The main hypothesis are that particles have high density, are packed in a sufficiently large number and the system is in a state of dense lumped mass. The resulting system might be modeled with a reduced number of Degrees of Freedom (DOF), where only friction and collision between particles and the enclosure are considered, hence particle interaction remains unaccounted (WANG; DAN, 2022).

Figure 11 – Computational model of additional single particle damper attached to the primary structure.

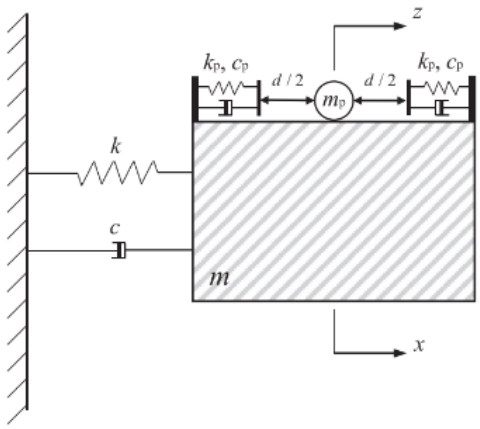

Source: Lu et al. (2020).

The afore mentioned method explicitly forsake the interactions between particles, what could limit the modeling of MPDs filled with powders. When modeling fine grains based MPDs, literature findings indicate that particles are highly influenced by fluid mechanics, affecting not only the kinetic energy but also the collision behavior (SáNCHEZ et al., 2012).

Meyer and Seifried (2020) identified five motion modes for steel particles ranging from powder 0.3 mm to spheres of 2.5 mm and 5 mm radius. The first mode was observed at low excitation intensities. It is characterized by a lumped mass behavior, with the relative velocity between particles tending to zero. As the excitation acceleration increases to 30 m/s^2, their behavior transitions from solid to fluidized motion; hence, establishing a threshold for the lumped mass model which encompasses the HAV vibration spectrum.

2.3 VIBRATION ANALYSIS

On it's simpler form, vibration monitoring can be performed by observing raw acceleration values over a period of time. Despite the relative low complexity, this method is useful for monitoring spikes of vibration and obtaining the VTV and DVE. Nonetheless, every single vibration analysis method relies on this primitive data form as it's raw material; hence, if abnormalities are observed at this point, preprocessing techniques must be implemented in order to acquire meaningful data.

In addition to storing acquired data, it is imperative to thoroughly document acquisition parameters. This documentation should include details such as sample rate, sensor sensitivity, measurement units, and any preprocessing techniques employed. Such information is essential for interpreting the acquired data accurately and ensuring that the measurement setup is capable of capturing the surveyed phenomenon effectively. Moreover, these setup parameters serve as crucial inputs for subsequent post-processing techniques which will be discussed on the subsequent sections. For instance the fixture which was used to limit the structure movements during testing will influence on the acquired modal parameters.

2.3.1 Spectral Analysis

Spectral analysis, or frequency analysis, is a technique designed to characterize time series data. Predominantly, the procedure involves acquiring measurements of acceleration, velocity or displacement with a known interval in between samples, preferably evenly spaced. Subsequently, the acquired data is decomposed into it's sinusoidal components via Fourier Transform where it's predominant frequencies are easily distinguishable.

The data acquisition stage consists of quantifying the structure response for a given excitation, hence it is crucial to understand the phenomenons under survey and how the data acquisition equipment works. The expected result of this step is a time series composed by acceleration, velocity or displacement measurements. Furthermore, the data acquisition constitutes the single most important step of the process due to the fact that once the acquired data is flawed the analysis as whole will be compromised, implementation details will be further discussed in section 2.4.6.

Both manual impact and vibration transducers may be used as excitation sources and theoretically yield the same result, nonetheless there are considerations to be made. Manual impact may exhibit less cohesion between impacts, yet it might not influence the structure's modal parameters. On the other hand, vibration transducers provide means for exciting the structure with a controlled signal, enabling frequency sweeps or random signals, while providing repeatability. However, their drawback lies in the potential influence on the structure's dynamic behavior due to mass loading and movement constraints (INMAN, 2014).

Once the appropriate force and acceleration time series are acquired, a signal analyzer is used digitize the analog time-domain measurements into digital frequency-domain information, with any variation of Fast Fourier Transform (FFT) algorithm.

In summation, this technique aids in discerning the amplitude and phase of each frequency component, contributing to a comprehensive understanding of the system's behavior. By examining the frequency domain, one can gain insights into resonant frequencies, damping effects, and potential modes of vibration.

The distinct advantage lies in the ability to precisely pinpoint and analyze the predominant frequencies, offering a more detailed and nuanced exploration of the dynamic behavior of a structure, as can be seen in figure 12, where a vibrating structure excited by a sinusoidal wave resonates on it's natural frequency.

Figure 12 – Acceleration curves presented in sequence: raw data, Power Spectrum, and Fourier Transform.

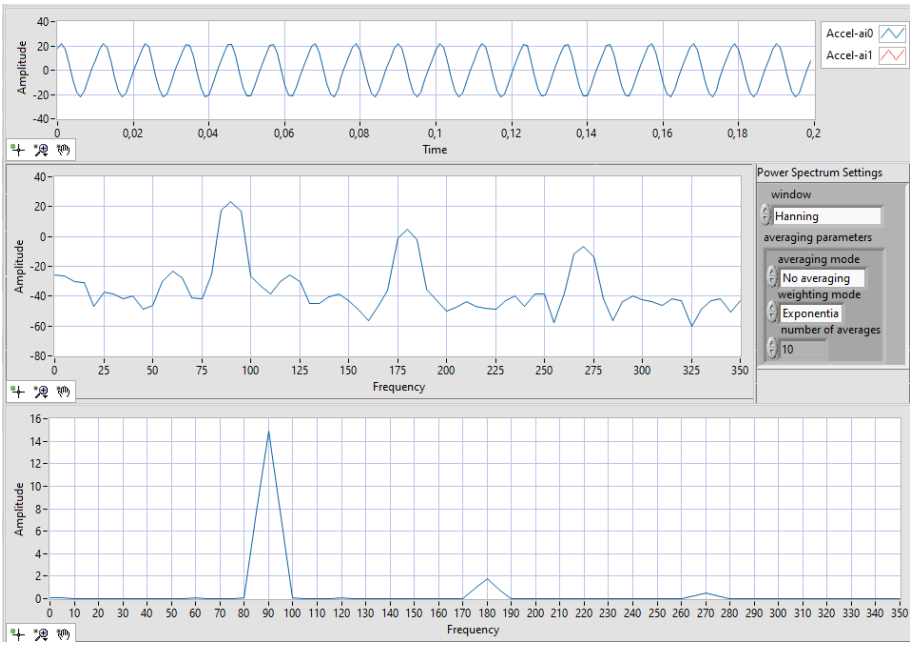

Source: Author (2024).

2.3.2 Experimental Modal Analysis

Modal analysis can be defined as the process of characterizing a structure's dynamic behavior. For simple structures, the modal parameters can be obtained by solving the equation of motion that defines the structure. However, in most engineering applications, defining this equation is far from a trivial task. Therefore, the field of EMA has developed several methods that can be categorized based on type of input data and numerical methods used. These categories include the sinusoidal input-output model, FRF, damped complex exponential response, and general input-output model.

The FRF methods are the most used, the main difference between the methods in this category resides in the Modal Parameter Estimation (MPE) algorithm used to process the FRFs into modal parameters. From the end user stand point, the method can be divided into three main steps, data acquisition, modal parameters estimation and interpretation of results (GATTI, 1999). EMAs can be performed with a minimum of two input channels, where one should capture the excitation and the other the response; thus, enabling the calculation of the FRF.

Once the experimental data is acquired, in this case the FRFs, the natural frequencies may be obtained by observation of the peaks of magnitude graphs or peaks of imaginary parts of the receptance or accelerance graphs, among other methods. During the MPE stage the user is often required to select the resonance frequencies through a consistency diagram (Figure 13).

Figure 13 – Consistency diagram

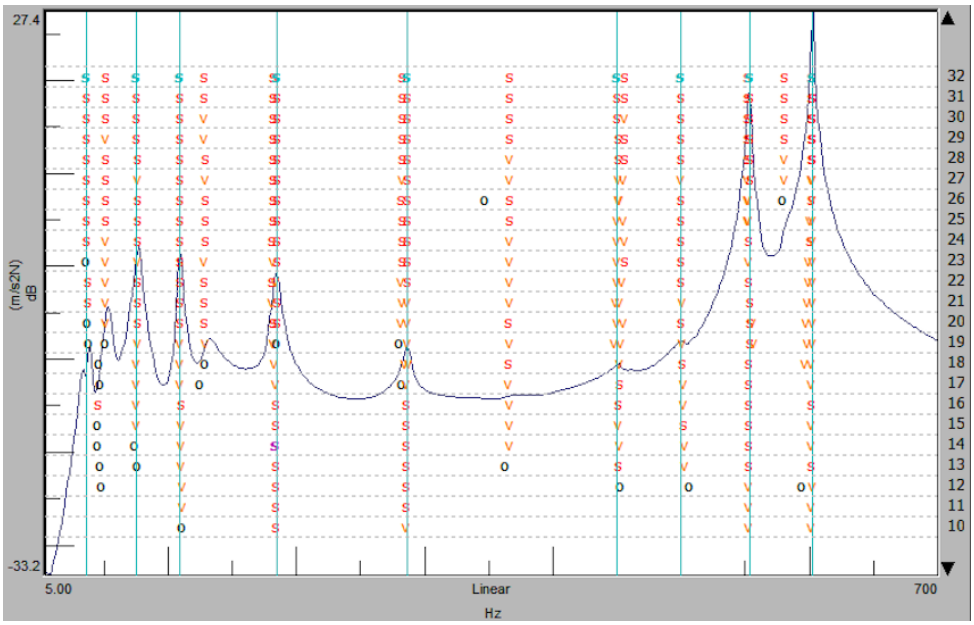

Source: Allemang and Brown (2022).

If the results are satisfactory, the software provides mode shapes, natural frequencies and damping coefficients of the structure. Additionally, an animation of the structure can be played, allowing for visual observation of its behavior. This visualization often provides more information than direct observation of the real structure, as it exaggerates the structure's movement through multiplier constants.

2.3.3 Operational Methods

The methods mentioned earlier may not always be applicable in real-world situations due to constraints on sensor placement and the ability to induce measurable excitation on the structure. Operational Modal Analysis (OMA) and Operational Deflection Shape (ODS) were developed to address these challenges by allowing the characterization of structures under real operating conditions (). As described by INMAN (2014), an ODS represents the vibration response from all modes of a structure combined and is typically studied in terms of modal parameters, most commonly mode shapes. These techniques serve as valuable diagnostic tools for detecting equipment damage and as direction for design improvements.

2.4 VIBRATION TESTING

As discussed on previous sections, defining the behavior of a structure is often a challenge, and every model has its limitations. Therefore, vibration testing plays an important role in characterizing structures' behavior and dynamic durability, as well as, validation of models. Due to it's nature, this field requires knowledge from several areas such as instrumentation and signal processing, as well as, vibration analysis addressed in section 2.3.

A generic Data Acquisition System (DAS) is composed by the excitation source, Device Under Testing (DUT), transducers, signal conditioners, signal analyzer and DAQ software (Figure 14). The capabilities of the hardware and software will dictate which vibration analysis can be performed. Each of these components have intricate relations and are available with specialized features for specific scenarios; hence, defining the experiment's requirements and constraints is critical for selecting appropriate components that are compatible with each other (INMAN, 2014).

Figure 14 – Schematic of hardware used to perform a vibration test.

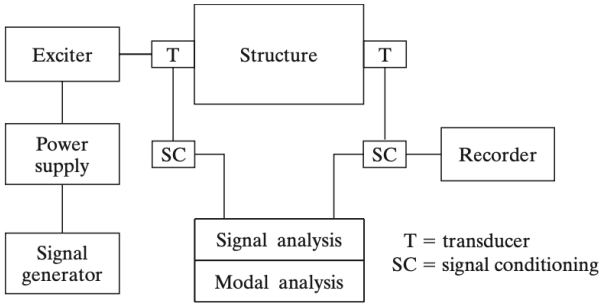

Source: INMAN (2014).

Initially the physical variables of interest should be defined and their characteristics should be accessed. For instance, their magnitude range, rate of change, environmental conditions, and duration will inform the selection of appropriate DAQ equipment. The definition of the sensor will provide requirements and constraints that must be attended by the remaining components.

2.4.1 Vibration Sensors

The selection of a vibration sensor must be made according to the properties of the phenomena under survey, once the minimal requirements are established the desirable sensor's characteristics can be defined. The essential sensor attributes are provided bellow:

- Sensitivity: represents the ratio between the input acceleration, velocity or displacement and the output of the sensor;

- Dynamic Range: stands for the region where the sensitive curve is approximately linear;
- Frequency Response: the upper limit defined based on the sensor's natural frequency and the lower limit tends to limited by the sensor's preamplifier.

The piezoelectric accelerometer is a type of seismic mass acceleration transducer and is the most commonly used vibration sensor since it's conception. In simple terms, it can be described as base excited single-degree-of-freedom systems, where the spring and the damper represents a piezoelectric element that produces charge once it is deformed by the movement of the seismic mass (Figure 15).

Figure 15 – Accelerometers configurations.

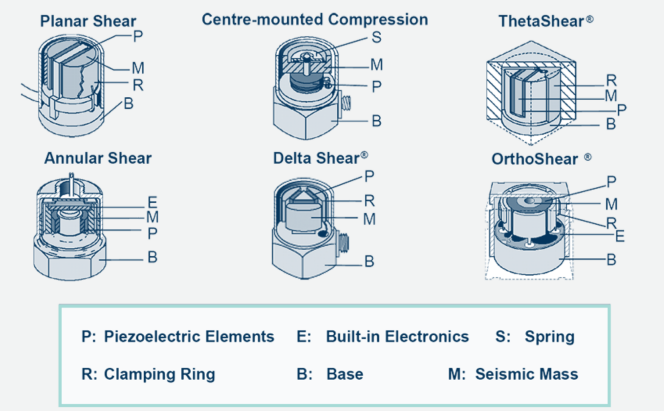

Source: Brüel & Kjær (2007).

The response curve of a generic piezoelectric sensor is shown in figure 16, the bottom end of the response curve is lower limit, while the dynamic range is the region with a flat response which is followed by an abrupt rise due to it's natural frequency. Generally speaking piezoelectric sensors have a damping ratio of approximately 0.03, hence the amplitude and phase are not modified until the natural frequency is eminent.

The operating range of accelerometers is constrained by mechanical and electrical factors. The upper limit is defined by one-third of the accelerometer resonance frequency for low damping designs, while the lower boundary is related to the type of preamplifier construction input voltage/charge. When a voltage amplifier is used, the lower boundary is a function of the system capacitance; in contrast, charge amplifiers do not disturb the output voltage due to cable length.

IEPE accelerometers are commonly used in vibration measurements, utilizing a method in which two wires from the transducer to the signal conditioning unit conduct both the power and the superimposed signal. Additionally, acoustic and vibration oriented DAS usually incorporate IEPE power, eliminating the need for a separate signal conditioner. This concept reduces the cost per channel and is less susceptible to cable length induced signal losses.

Figure 16 – Useful operating range of piezoelectric transducers.

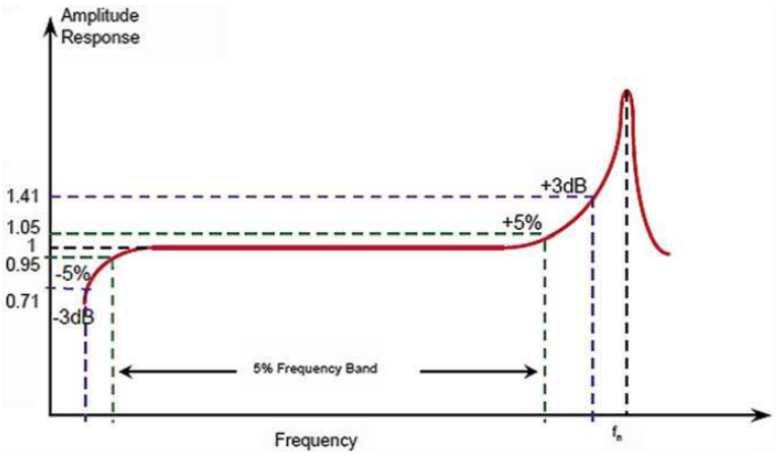

Source: Allemang and Brown (2022).

For frequencies under 2000 Hz, the mounting technique is not critical. However, caution must be taken to avoid ground loops with the structure under survey. Attachment methods differ by their resonance frequency and can include threaded steel studs, cement, wax, and even magnets for low-frequency applications.

2.4.2 Vibration Generators

For EMA, the fundamental objective of an excitation source hardware is to be capable of exciting all structure's modes of interest, while inducing minimal disturbance in the structure's behavior. Artificial input methods can be categorized into impulsive or controlled inputs. Impulsive inputs induce a transient excitation by impact hammers, step relaxation or some sort of short duration input. Controlled inputs, on the other hand, can induce deterministic or random signal that may be used perform frequency sweeps, single tone or to mimic operational loads.

Impulse hammers, or impact hammers, are devices equipped with a built-in force transducer. They can be fitted with different tips and adjustable hammerhead masses, allowing control over the resulting impact force and the cutoff frequency of the impulse.

The term shaker refers to electromagnetic or electrohydraulic devices capable of inputting signals to a structure. These can include electric motors with an unbalanced mass attached to their rotor, linear voice coil actuators, or any actuator capable of inducing a force that satisfies the test requirements. The DUT may be mounted on to the shakers' platform (Figure 17) but usually are coupled to through stingers. Stingers not only provide more precision in the force application point but also help mitigate mass loading effects (ALLEMANG; BROWN, 2022).

Figure 17 – Single side of two piece handlebar fixed to electrodynamic shaker.

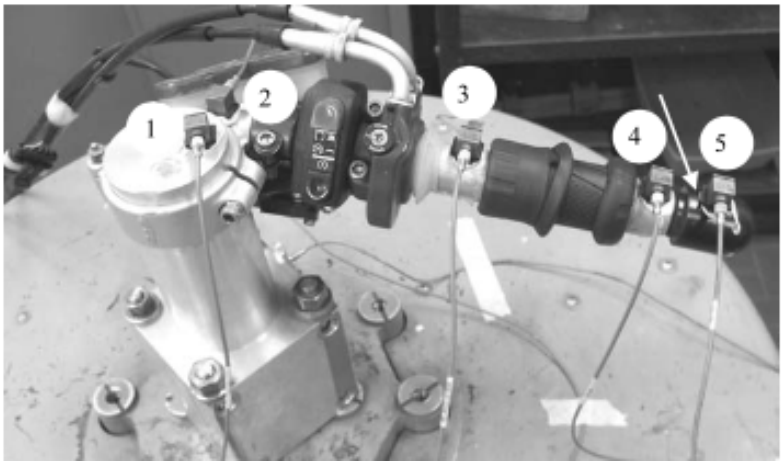

Source: Fasana and Giorcelli (2010).

To define the appropriate excitation source, the moving mass of the DUT and the maximum acceleration or force should be estimated. Once these parameters are determined, it is a matter of selecting or developing a force transducer that meets these requirements. Moreover, except for impact hammers, exciters require additional hardware to operate, including signal generators, signal amplifiers and sensors to quantify the excitation input to the structure.

2.4.2.1 Excitation Signal

When the excitation source is provided by a shaker, there are four common types of excitation signal single sine wave, swept sine, random noise or pseudo-random noise. The first two offer the higher signal to noise ratio but take more time to cover all the frequencies of interest when compared to the last two.

Single sine was the dominant excitation pattern for vibration testing, one of the reasons for this dominance was the lack of computational power to generate more complex signals. It's excitation input consists of applying a harmonic force of constant magnitude at a variety of different frequencies, ranging from a small value to larger values covering a frequency range of interest. At each step, the DUT is allowed to reach steady state before the response is measured. The difference for the swept sine technique is that the frequency sweep is governed by a sweep rate, which should be slow enough to not disturb the frequency response of the structure.

With the advancement of DAS and the capability to generate random noise, many industries have opted for this type of excitation input since it provides more realistic testing for various use cases. Random vibration is defined as a signal whose details are not available beforehand, requiring analysis in terms of their statistical properties such as average, Root Mean Square (RMS), and PSD.

Pseudo-random noise is characterized by having a random amplitude over a fixed set of frequencies, while in random noise both frequency and amplitude are random. The later is subjected to Leakage due to the fact that the spectrum analyzer won't be able to represent the complete spectrum of the random signal. In practice, vibration testing is generally conducted with band-limited pseudo-random noise as shown in figure 18.

Figure 18 – PSD in terms of acceleration from random vibration test standards.

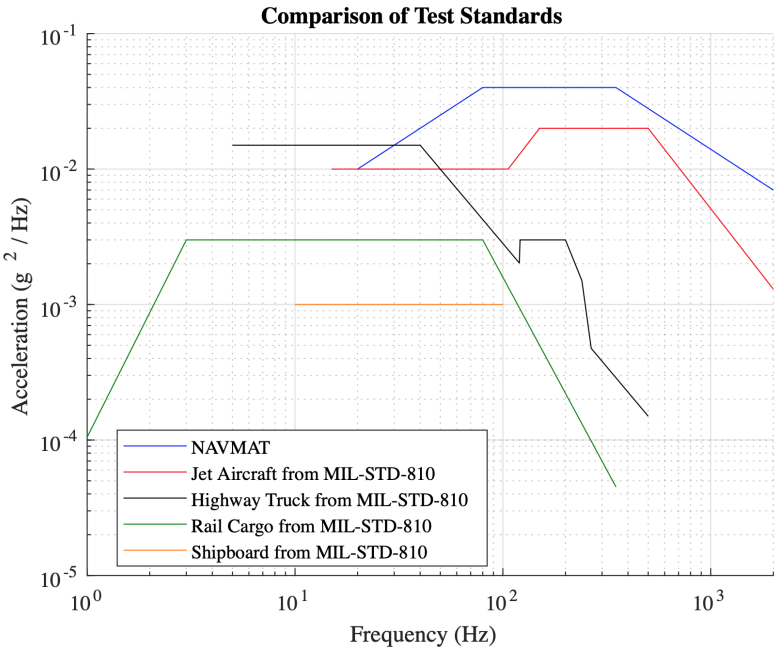

Source: Hanly (2020).

2.4.3 Signal Conditioners

Signal conditioners are essential analog devices that interface between the sensor and the Analog to Digital Converter (ADC). The choice of signal conditioners is determined by the sensor type and the specific requirements of the measurement task. For instance, piezoelectric sensors typically necessitate charge amplifiers, while IEPE sensors require constant current power supplies.

Along their main functionalities, these devices may contain signal amplifiers to adjust the sensor output voltage to the specifications of the DAS' inputs. As well as, impedance buffers that mitigate signal attenuation due to long cable lengths or low resistive load, which may damage the sensor's electronics. Finally, some type of filtering is required to prevent aliasing and improve the signal to noise ratio (ALLEMANG; BROWN, 2022).

2.4.4 Data Acquisition System

The DAS provides an interface between the conditioned data and the user. These devices, are tasked with converting conditioned analog signals into digital data which may be processed, displayed or achieved, depending of the device capabilities. Modern devices, often provide Universal Serial Bus (USB) communication therefore a computer may be used as signal analyzer. This integration reduces costs and enhances the versatility.

As every acquired signal must be digitized through an ADC in order to be stored, processed or displayed by digital systems, the basic requirements for defining the appropriate hardware are tied to the acquired signal characteristics and are provided below:

- Clock speed: usually measured in Hertz, it will limit the maximum sample rate;
- Input/Output (I/O) Full Scale Range Voltage: maximum and minimum voltage that the I/O supports;
- ADC/Digital to Analog Converter (DAC) Number of bits: defines the available resolution, which may be calculated as:

$$Resolution = \frac{V_{FSR}}{2^n} \tag{3}$$

  Where V_{FSR} stands for Full Scale Range Voltage and n is the number of bits;
- Number of I/Os;

Apart from the minimum requirements, once the scope of the experiment is defined, the selection of the DAS depends on factors such as available budget, storage capacity, modularity, software compatibly, embedded signal conditioners, data transfer interface and environmental constraints.

2.4.5 Data Acquisition Software

Data acquisition software serves as the interface between DAQ hardware and the user, enabling the setup, control, and monitoring of the entire system. The software allows users to configure sensor settings, adjust signal conditioning parameters, and define data logging protocols. It provides real-time feedback, displaying signals as they are being recorded, which helps in immediate identification of any issues during the acquisition process. DAQ software often includes features for automated data processing, such as event-triggered recording and alarm generation based on specified conditions. The choice of software is influenced by the complexity of the tests, the required data processing capabilities, and the user interface's ease of use. High-quality DAQ software enhances the efficiency and effectiveness of vibration testing by streamlining the data acquisition and analysis process.

Despite complete solutions, quite often DAQ software is developed for specific applications through the Laboratory Virtual Instrument Engineering Workbench (LabVIEW) and python algorithms.

2.4.6 Measurement Data Validation

The measurement process is inherently susceptible to various sources of error, ranging from incorrect acquisition parameters to random noise. While achieving complete accuracy is desirable, for most applications recognizing error sources is sufficient once a minimal threshold is achieved. As stated by Randall et al. (2020), "One of the principal aims of signal processing is to extract information from non-ideal measurements." Given that an error is defined as a deviation from the expected value, mapping these error sources is essential for a thorough understanding of the acquired data.

Before conducting any experiment, the DAS should be evaluated as a whole to assess the quality of the acquired data. First and foremost, the acquired time domain data must be observed to identify the following anomalies:

- Aliasing: misinterpretation of a higher frequency due to inadequate sample rate. The Nyquist criterion establishes that the sample rate must be greater than twice the highest frequency of interest, although it is recommended to acquire at five to ten times the highest frequency of interest (ABU-MAHFOUZ, 2022).
- Leakage: phenomenon associated with the lack of frequency resolution, resulting from the finite time window used for the computation of the FFT;
- Clipping: acquired signal is limited due insufficient input scale range;
- Random noise: although it is expected it should be kept at an order of magnitude lower than the signal of interest;
- Narrow-band noise: may occur due to improper shielding or isolation from Alternate Current (AC) power source;
- Improper sensor mounting may result in a nonlinear impedance.

One effective method for this evaluation is calibration through comparison. This process involves comparing the measurements obtained from the DAS with those from a known reference or standard. Discrepancies between the DAS and the reference measurements can highlight inaccuracies or biases in the system, allowing for adjustments and improvements.

An integral part of vibration analysis resides in the frequency domain data computed, therefore, this data should also be verified and adjusted beforehand to prevent digital signal processing errors such as leakage. Leakage is a phenomenon caused by the truncation in time that occurs for continuous signals which are not periodic in N, when we limit the calculation of the Discrete Fourier Transform (DFT) to N samples (ALLEMANG; BROWN, 2022).

2.5 STATE OF THE ART

Whilst validating MPDs, it is essential to characterize the dynamic behavior of the DUT with and without the influence of the absorber. Despite this common requirement, experiments in literature have been conducted either with a complete motorcycle or with isolated components. Testing a complete motorcycle enables using the engine as the excitation source, which in turn might provide results that better represent real-world conditions. Although, several drawbacks must be considered, particularly cost and the elevated complexity involved in modeling, data acquisition, and general infrastructure. On the other side, testing isolated components greatly simplify the modeling process of the test setup, but imposes the use of an artificial excitation source.

Podosek et al. (2022) developed a full-scale test bench whose actuators are adequate to excite fully-assembled motorcycles, and verified it's capabilities. A similar approach was undertaken by Chindamo et al. (2017). Although these studies are capable of analyzing a complete motorcycle, the resources needed for such test stands are immense. Simpler approaches have achieved valuable results, as demonstrated by Cheli et al. (2011) and Khune and Bhende (2020), who employed complete motorcycles but evaluated only the vibrations resulting from the combustion engine.

Under the assumption that engine unbalance is the main source of HAV, Khune and Bhende (2020) conducted a design of experiments (DOE) to develop a TMD for a motorcycle handlebar. The experiment was conducted with the complete motorcycle supported by it's on stand and all components mounted on the handlebar were removed and tested in batches in order to have a better understanding their influence on the handlebar's dynamic behavior. To maximize the vibration source the chosen motorcycle for the experiment was equipped with a under square single cylinder engine. The authors instrumented the handlebar with a single-axis IEPE accelerometer positioned at the handlebar's extremity. The acquired data was processed using the National Instruments (NI) LabVIEW software and lead to the conclusion that the proposed TMD was effective.

Bertozzi et al. (2022) developed a setup for accessing perceived discomfort due to handlebar vibration, it consisted of a electrodynamic shaker (LDS V930) capable of producing 105 kN of force attached to the handlebar. Moreover, Inertial Measurement Units (IMUs) were used to measure human-body angles, a Laser Doppler Vibrometer (LDV) and a ceramic shear accelerometer (333B30 PCB) were used for measuring the velocity ratio between the hand and the shaker head.

3 METHODOLOGY

This chapter is structured to address the critical aspects of developing a vibration test bench aimed at validating vibration absorbers. It begins with an assessment of the test bench requirements, detailing the criteria for selecting hardware components such as sensors, vibration generators, and DAQ systems. Following this, it discusses the experimental setup development, including the design and assembly of the test bench structure and DAQ parameter estimation. This comprehensive approach ensures an integrated and efficient methodology for the development of the test bench, followed by a well-founded verification of the MPDs.

3.1 TEST BENCH REQUIREMENTS ASSESSMENT

In order to define the requirements for the test bench and gain knowledge over the dynamic characteristics of a handlebar, a ODS was conducted in site with a complete motorcycle. Later on, the handlebar was disassembled and two modal analysis were conducted to comprehend the influence of different fixtures. As previously stated (Chapter 2), both vibration analysis methods provide valuable information regarding the natural frequencies, mode shapes and further dynamic characteristics of the DUT, which are crucial information for the selection of appropriate sensors, DAQ and vibration generator.

3.1.1 Operational Deflection Shape Analysis

The procedure was conducted on a complete motorcycle equipped with a single-cylinder over-square engine with a capacity of 310 cubic centimeters. The engine is directly mounted to the tube frame, hence increasing the impedance between engine block and the motorcycle tube frame. Despite the factory-installed counterweights placed at both ends of the handlebar, this model lacked any additional devices with specific intent of reducing vibrations beyond its suspension.

During the acquisition, the motorcycle had both tires on the ground and was balanced by it's kickstand, which was placed over riser pads. Leveling the motorcycle, reduces the weight transfer towards the left side of the motorcycle chassis, therefore, balances the weight distribution, as well as minimizes the disparity among the accelerometers' readings due to the angle difference between the left and right side of the handlebar. The acceleration was acquired through the Brüel & Kjær(BK) LAN-XI DAQ module with two Brüel & Kjær triaxial accelerometers placed along the handlebar in vertical orientation, one of them was fixed and the second was placed in new position after each measurement until all position were covered.

The distances were measured from the accelerometer center with a measuring tape and a geometry was modeled on the BK Connect software. The accelerometers were attached using instant adhesive and white ink was applied to mark the measurement points, improving repeatability for potential future data acquisitions (Figure 19). Finally, the source of vibration for the experiments was the running engine at idle, which is close to 1500 RPM, and 2500 RPM, with gearbox on the neutral position.

Figure 19 – Similar approach used for accelerometer placement.

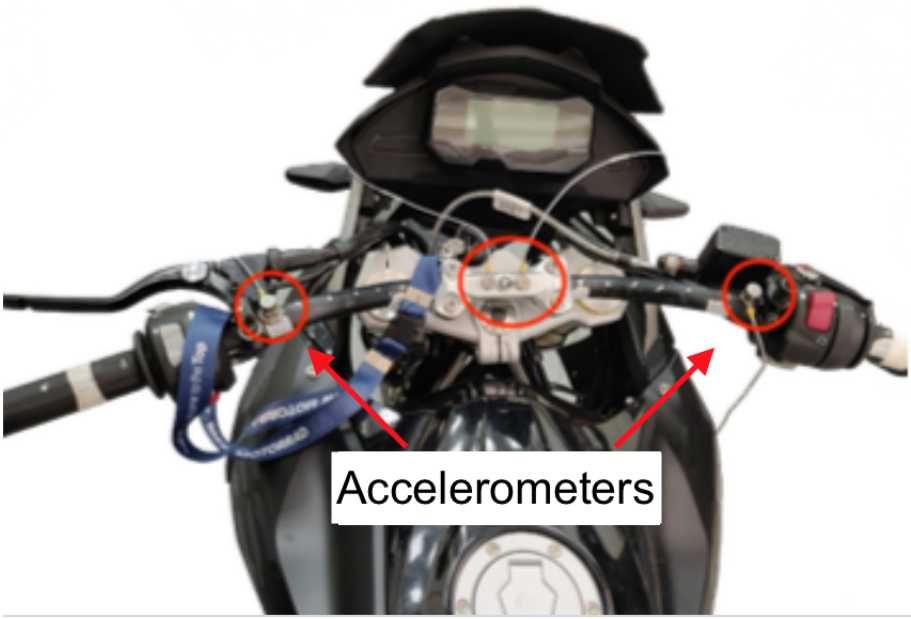

Source: Author (2023).

A complete motorcycle handlebar unit includes various components such as grips, throttle, clutch lever, brake lever, switch-gear, mirrors, master cylinder, and bar ends. Although only the bar ends are explicitly used as a vibration control device, all components interact with the vibrating structure, thereby altering the dynamic behavior of the handlebar and the motorcycle. Both trials were conducted with a fully assembled handlebar and the predominant frequencies found are displayed in table 3. Additionally, the ODSs for the 2500 RPM trial are displayed in figure 20.

Table 3 – Predominant frequencies for each trial.

Frequency [Hz]	
1500 RPM	2500 RPM
33	84
146	120
	232

Source: Author (2024).

Figure 20 – Operational Deflection Shapes found at 2500 RPM.

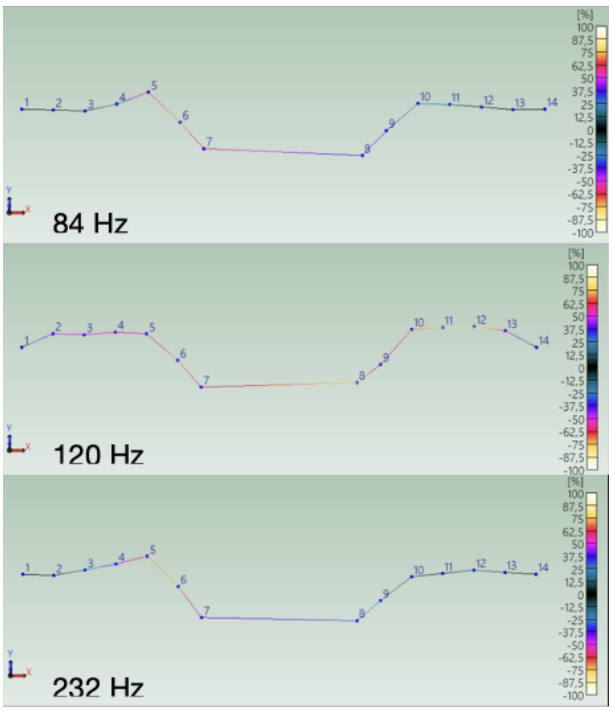

Source: Author (2024).

3.1.2 Experimental Modal Analysis

As pointed out on the section 2, one of the most common configurations is suspending the structure with light weight cords, which simulates an unrestrained condition. For the purpose of defining the test bench geometry through a better understanding of the fixture influence on the DUT, an EMA was conducted with a suspended handlebar. The experiment was conducted with the LMS Pimento Signal Analyser, the accelerometer employed was the Kistler 8702B500 and the Brüel & Kjær Impact Hammer Type 8206 equipped with a aluminium tip (DB-3991-001). The sensitivity for the hammer and accelerometer was set to 19 mV/N and 10,0 mV/g respectively, according to the calibration chart provided by the manufacturers.

The DUT was marked at 14 points using white ink, and the accelerometer was positioned at the fourteenth point for all of the impacts. For each point, two impacts, averaging 25 newtons, were acquired. The acceptation criteria for the measured values was primarily based on the quality of the hit meaning that the hammer should touch only once at the structure, which can be observed by the force measured through the impedance head embedded in the hammer head. Additionally, for the second hit the calculated coherence should remain higher then 0.7 around the resonance frequency. The structure consisted of the handlebar clamped to the vibration generator support, along with the vibration generator, a similar configuration can be observed in figure 21.

The DUT was supported by synthetic fiber strings positioned 5 cm from each end and had no additional components attached. While the additional mass of the support and vibration generators did influence the dynamic response, the primary goal of these experiments was to collect data that closely resembled the test bench conditions. The FRF obtained from the suspended configuration is shown in figure 22.

Figure 21 – Handlebar supported by flexible cords.

Source: Author (2023).

Figure 22 – Frequency response of the handlebar in Free-Free condition.

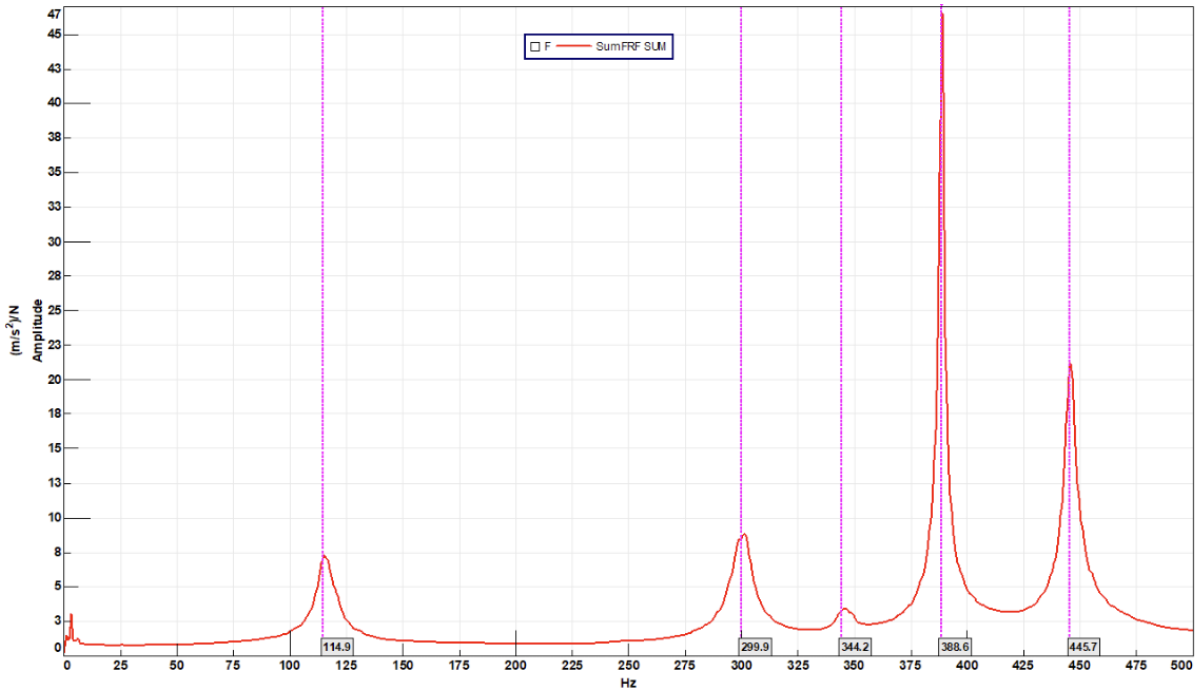

Source: Author (2024).

3.2 DATA ACQUISITION SYSTEM

Upon compiling and comparing the results of preliminary experiments with published data, all fundamental requirements for the test bench were established. Any remaining requirements are contingent on sensor outputs and will be addressed in subsequent sections of this chapter.

3.2.1 Sensors

The minimal sensor requirements in order perform a spectral analysis would be any transducer that is capable of measuring acceleration, velocity or displacement. The accelerometer was selected due to the practicality of measuring the desired quantity directly, for the wide frequency range it provides and finally due to it's compact and light form factor.

The specific sensor chosen was the uni-axial piezoelectric accelerometer Kistler 8702B500 (Figure 23), which is designed for general purpose vibration measurements and is capable of measuring accelerations up to 500 $\frac{m}{s^2}$ which is at least 50 times the required magnitude for this application. It's resonance frequency is close to 10 kHz and the lower frequency limit of 0.5 Hz provides the necessary frequency band required for vibration measurements. Additionally, it has a constant current internal amplifier that contributes for lower electromagnetic interference due to extensive cable lengths, and outputs a maximum of 5 Volts.

Figure 23 – Kistler 8702B500 uni-axial accelerometer

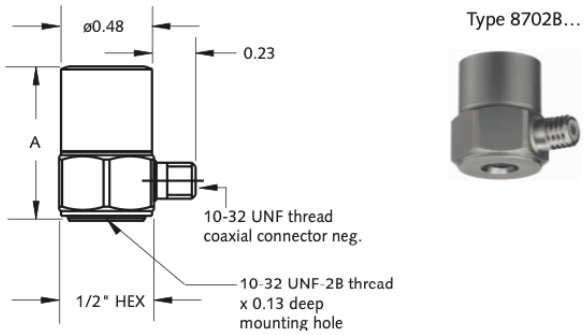

Dim.	Type 8702B500...	Type 8702B500M1, M3	Type 8702B500M5 / M8
A	0.63	0.67	0.80

Source:

Both accelerometers were placed vertically and secured with liquid adhesive, while one of them was placed on the center of the handlebar, as close as possible to the excitation source. The second one was placed at 1 cm from the handlebar extremity, in order to capture maximum acceleration magnitudes. This configuration had been previously validated during the modal analysis experiments and assures the sensors are not placed in any of the nodes of the frequencies of interest.

3.2.2 Vibration Generator Components

Ideally, a purpose-built vibration generator for laboratory use, equipped with embedded sensors and robust against electromagnetic and mechanical interference, would be the preferred option. However, low-frequency speakers present an extremely cost-effective alternative that has not been thoroughly explored yet. Consequently, the Buttkicker LTE low-frequency speaker, designed for vibrating small platforms and furniture, was selected for this study. It offers a frequency response ranging from 5 Hz to 350 Hz and a power capacity of up to 250 watts, making it suitable for generating the required vibrations within the desired frequency range.

The same considerations apply to the sound amplifier. The primary concern was selecting equipment that could provide the necessary frequency range while being cost-effective relative to the chosen vibration generator. The Taramps TS400x4 automotive sound amplifier was selected due to its acceptable frequency range of 18Hz up to 30KHz, power of 400 Watts and input voltage of 12 Volts DC that offers the possibility of performing off grid experiments that might avoid interference from the 220 VAC supply voltage of the laboratory.

As the power source for the sound amplifier a 12 Volts battery was used to establish a reference and was replaced by a Switched-Mode Power Supply (SMPS) rated at 12 Volts DC 250 Watts. The comparison between the power sources did not justify the effort of charging the battery because the noise from the SMPS was negligible.

3.2.3 Data Acquisition Hardware

In defining the initial considerations for the DAQ hardware, the primary focus were the minimum requirements for each component and the secondary were environmental constraints, given the intended placement within a controlled laboratory setting. As such, there was no need for the system to withstand outdoor conditions or facilitate transport during data acquisition. Therefore, portable and weather-resistant equipment was not considered.

Additionally, standalone DAQ hardware often come with higher costs, which did not align with the budget for the test bench project. Hence, the system was designed to be used in conjunction with a computer. Specifically, the decision to avoid a Peripheral Component Interconnect (PCI) board configuration was intentional, as it would require the use of a designated desktop computer while devices with native USB may be connected to any computer that fulfills it's minimum requirements.

From this point of view, the NI USB-4431 was selected based on the fulfillment of the minimum requirements (Table 4), the compatible cost and due to it's versatility since it has native USB compatibility and it's inputs are compatible with IEPE sensors.

Table 4 – DAQ system minimum requirements.

Requirements	Value	Units
Number of Analogue Inputs	2	-
Number of Analogue Outputs	1	-
Sample rate	3,5	kS/s
Resolution	16	bits
Input Range	+-10	V

Source: Author (2023).

Moreover, NI provides a free of charge license for students for their LabVIEW software, which is graphical programming environment for test systems development. At the lowest level of it's the complexity the software enables controlling the hardware acquisition parameters as well as storing the acquired data. Although it's capabilities extend to processing, visualizing and generating data, through numerous features.

3.3 TEST BENCH STRUCTURE

The primary objectives were to create a robust structure that allows for testing various handlebar appendices while minimizing the influence on the handlebar's dynamic behavior. A stable and sturdy setup reduces variations in experimental conditions, thereby decreasing measurement errors and enhancing data reliability across multiple experiments.

In order to minimize the influence of the test bench on the handlebar's dynamic behavior the test bench structure should be designed in such a way that it's natural frequencies are distanced from those of the handlebar, which in practical terms means that the supporting structure must be as rigid as possible or as light as possible. The first option can be achieved by proper material selection, as for the later, it can be obtained by supporting the structure with flexible cords. The dynamic behavior should be consistent with the observations made in the motorcycle and in the suspended handlebar configuration. This requirement ensures that the test bench does not introduce significant artifacts that could distort the handlebar's behavior.

During the development process of the supporting structure, three different fixture configurations were tested. The first configuration involved suspending the handlebar with flexible cords. This method was cost-effective and allowed the DUT to move freely, achieving a free-free EMA configuration. However, it restricted testing with handlebar appendices due to the collision of the cords with the side-view mirrors and hand controls (Figure 21).

The second configuration tested involved attaching the handlebar to the shaker using the same fixture as the previous experiment. Although, instead of suspending the DUT, the structure was supported by a dense foam, as depicted in figure 24.

Figure 24 – Foam test bench

Source: Author (2023).

This setup yielded results similar to the first, but would often result in low coherence in between trials, due to the lack of restraints keeping the DUT in the same position. The handlebar movement and the foam's spring-like behavior compromised repeatability and resulted in multiple vibration modes that were indistinguishable; thus, compromising the analysis of the dynamic behavior of the DUT.

The final configuration of the test bench (Figure 26) aimed to enhance measurement coherence and define handlebar vibration modes clearly, by distancing the test bench's resonance frequencies from the DUT ones. The structure's foundation is composed by a 70 kg concrete block, which is used to anchor rubber bushings that isolate the test bench from environment disturbances. On top of bushings, a 2.74 kg circular steel plate is placed as the base for the remaining components (Figure 25). The handlebar is attached to the shaker by two 105 g aluminum blocks and a 200 g stainless steel circular plate, which are fastened to the steel plate and weight 4.835 kg in total. Additionally, the use of rubber bushings in the final configuration had the intent of isolating the handlebar from external vibrations. At first only three rubber bushings rated for 70 kg were used and a second trial was performed with nine rubber bushings.

The manufacturing process involved drilling holes in the concrete block, cleaning it thoroughly to remove any dust, applying chemical anchor until one-third of the hole was filled, and then screwing the bushing into place. However, potential inaccuracies in the drilling process caused the bushings to be bonded at a slight angle from the vertical axis center, effectively acting as springs and introducing disturbances to the dynamic behavior of the DUT. The proposed solution was to increase the number of rubber bushings in order to increase the system rigidity while reducing influence of bushings' misalignment.

Figure 25 – Circular steel plate with nine bushings attached to it.

Source: Author (2024).

Also the third setup was the first to respect the recommended distances between equipment to mitigate electromagnetic interference between the host computer monitor, power source and shaker from the DAQ.

3.4 EXPERIMENTAL SETUP

In addition to hardware selection and test bench assembly, the experimental setup involved multiple configurations and trial runs aimed at mitigating common measurement errors. Initially, the test bench was thoroughly inspected to ensure that all cables were properly connected, fasteners were tightened, and accelerometers were correctly positioned.

Signal acquisition literature does not provide universal acquisition parameters but rather guidelines that serve as estimations. Therefore, following the hardware verification, a parameter estimation was conducted based on these initial guidelines. Multiple trials were performed to validate the results obtained with different acquisition parameters, including sample rate, frequency resolution, averaging parameters, and excitation signal properties.

According to the Nyquist Theorem, the acquisition frequency should be at least twice the highest frequency of interest. However, in practice, most sources recommend a sampling frequency at least five times greater to ensure more accurate data capture and reduce aliasing effects (ALLEMANG; BROWN, 2022). A Brüel & Kjær calibration exciter type 4294 was used to verify the acquired data; once the acquired signal matched the expected values, the experimental setup was fixed for the entire duration of each experiment.

Figure 26 – Test bench hardware setup.

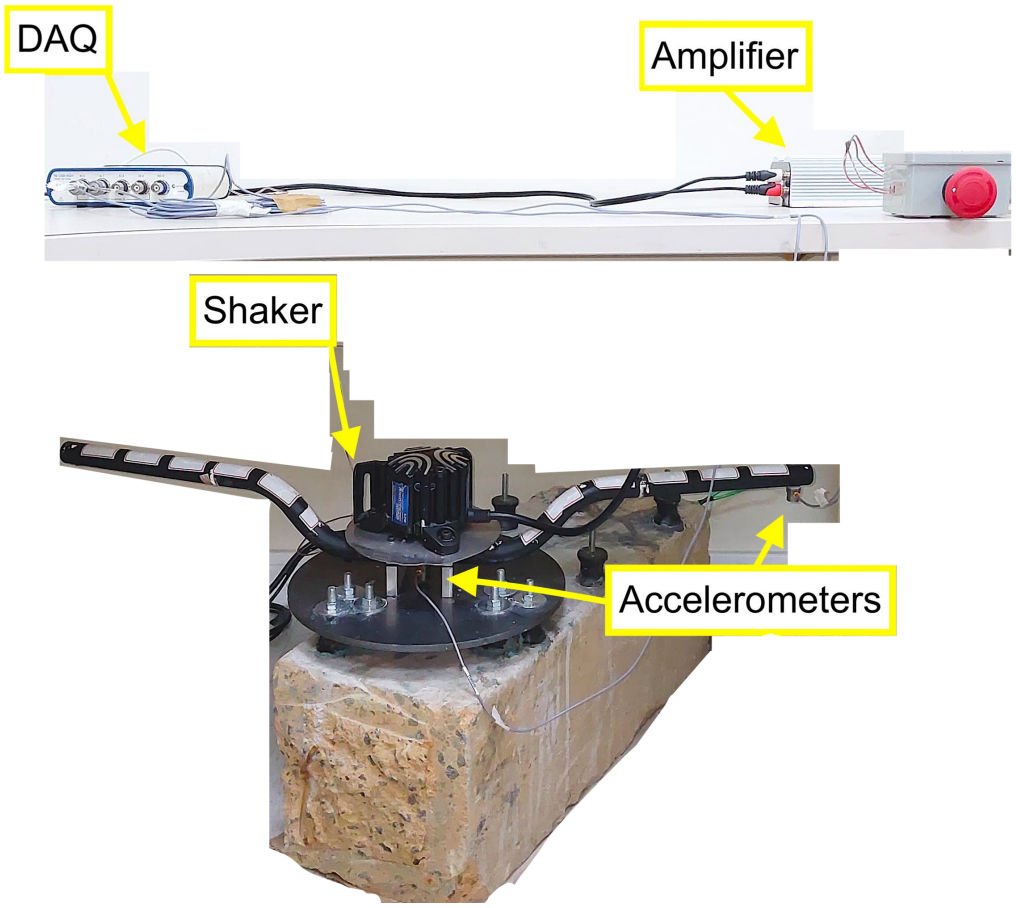

Source: Author (2024).

Under these conditions, exploratory experiments were conducted, with their acquisition parameters presented in Table 5. To mitigate spectral leakage, the Hanning window function was implemented for each experiment, which is standard for random signals and spectral density estimates. Additionally, to minimize uncertainty and improve the signal-to-noise ratio for the response signals, the frequency response was computed by taking 20 averages per FFT computation.

Table 5 – Acquisition parameters for MPDs verification.

Parameter	Experiment		Unity
	One	Two	
HW Sample Rate	1200	50000	S/s
SW Sample Rate	600	25000	S/s
FFT Averages	20	20	-
FFT Window	Hanning		-
FFT Frequency Resolution	5	2	Hz

Source: Author (2024).

3.5 MULTIPLE PARTICLE DAMPERS

The verification of the MPDs was performed using the same enclosure (Figure 27), which consists of a machined aluminum cylinder whose relevant characteristics are compiled in table 6.

Figure 27 – MPD enclosure filled with rubber and factory counterweight.

Source: Author (2024).

Table 6 – MPD's enclosure physical characteristics.

Parameter	Value	Unity
Total mass	121	g
Internal Volume	0.0284	mm^3
Internal Diameter	42	mm
Wall thickness	2	mm

Source: Author (2024).

All experiments conducted aimed to compare the response of the handlebar to a band-limited white noise excitation, with the cutoff frequency set to 350 Hz due to the shaker frequency response limitation. The variations among the experiments lay in the different configurations of the MPD attached to both ends of the handlebar.

The first experiment was carried out with six distinct configurations: the handlebar alone, the handlebar with factory counterweights, the MPD's enclosure empty, and the MPD filled with barite, magnetite or an undisclosed polymer (FIMO) at a 90% filling rate. The mass of each configuration is compiled in table 7.

As for the second experiment, the mass was fixed for all materials based on the least dense one. Additionally, a non-particulate lumped mass was used to determine if the attenuation was solely caused by the mass increase. Since FIMO was the least dense compared to the other materials, the mass corresponding to a 90% filling rate with FIMO was used to compare all materials with 28 g of particle mass, which results in a fixed total mass of 149 g for each absorber (Figure 28).

Table 7 – Total mass of each absorber configuration for a 90% filling rate.

Material	Total Mass [g]
Counter Wight	221
Empty Enclosure	121
FIMO	148
Synthetic Rubber	140
Magnetite	190
Barite	190

Source: Author (2024).

Figure 28 – Particles used in experiments one and two.

Source: Author (2024).

4 SOFTWARE

For achieving the goal of verifying dampers' efficiency, the DAQ software must fulfill several critical requirements. These requirements include controlling the test bench electronic hardware, processing the collected data, displaying the data in a user-friendly manner and enabling effective user interaction. This chapter will detail the development and implementation of the DAQ software, discussing its architecture, key functionalities, and the rationale behind its design choices.

For all tasks to be performed in a synchronized manner while enabling user interaction with the software, the system is divided into modules with unique responsibilities (Figure 29). Each of them is a Virtual Instrument (VI) that implements a state machine, whose state is defined by the messages received by the main VI. The messages may contain data or instructions for sending messages to other modules or performing tasks. In this way, the system can perform multiple tasks at once in a non-blocking manner.

Figure 29 – DAQ software outline.

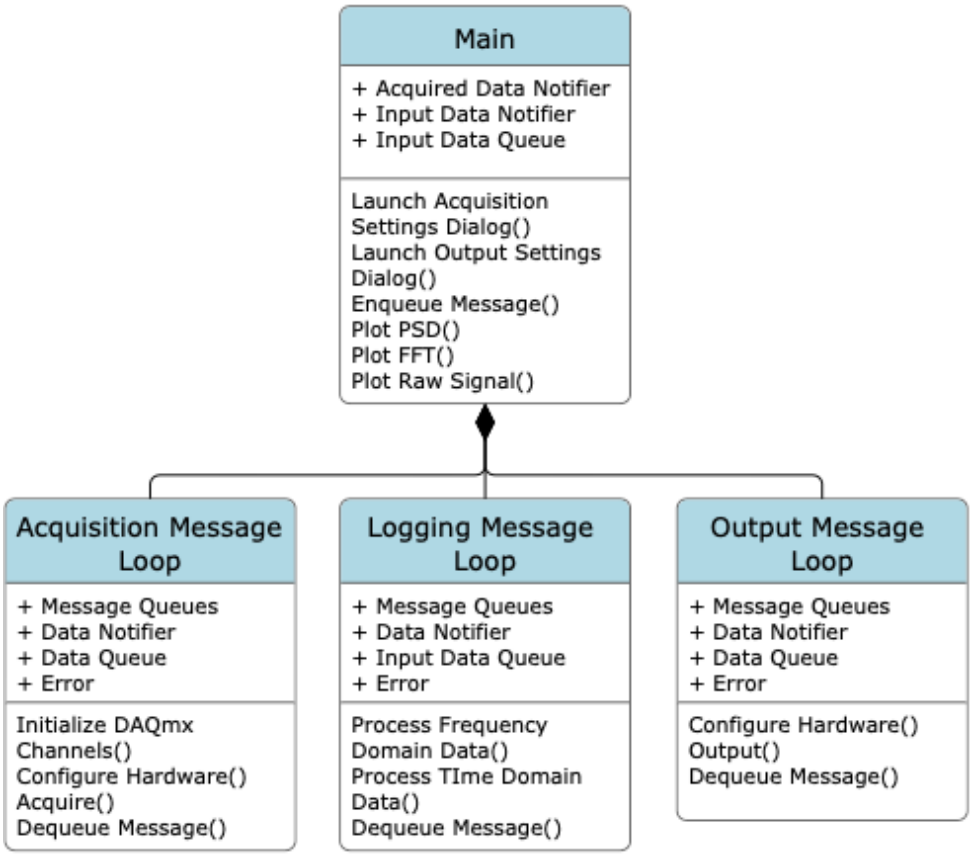

Source: Author (2024).

Figure 30 – Systematic process for assessing the effectiveness of MPDs.

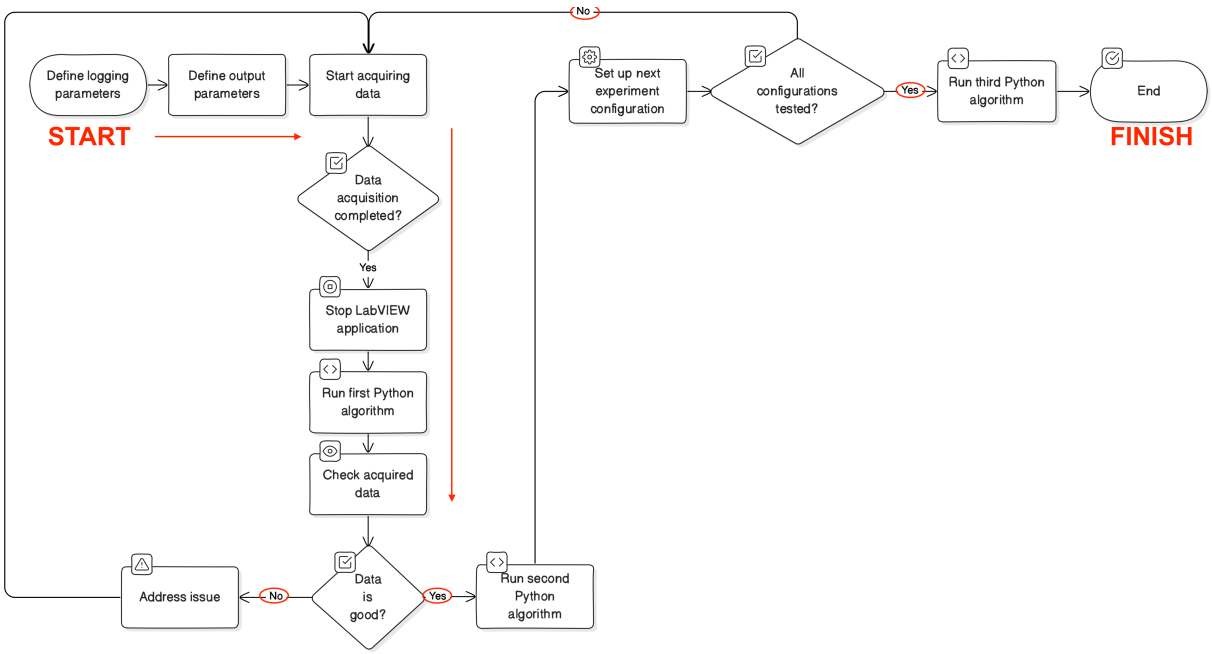

Source: Author (2024).

The basic concept is that the communication is performed through messages that are generated in the main module and distributed across the other modules. This messages may contain structured data such as raw values from the accelerometers with their respective timestamps or may contain instructions for controlling the state of the module it is addressed to. Once the main module is started a initialization message is dispatched to all sub modules. Each module can return messages to the main module, ensuring information persistence across all modules.

Once the experiment is completed and the data is logged in structured text files, a post-processing algorithm written in Python generates figures to identify and discard any inconsistent or erroneous data promptly. After filtering out the bad runs, a second algorithm is used to generate figures that compare the test runs for a specific test setup, returning the mean values of all FFTs computed for each run. Finally, a third algorithm compares all the different test setups, facilitating the comparison of the various scenarios analyzed.

The experiment workflow, illustrated in Figure 30, outlines the systematic process for assessing the effectiveness of MPDs. It begins by setting logging and output parameters, followed by initiating data acquisition. After completing data acquisition, the LabVIEW application is halted. Subsequently, Python algorithms are employed to evaluate data quality and gather statistical insights for each scenario. This process iterates for all configurations, culminating in a comprehensive comparison of collected data using the third Python algorithm.

4.0.1 Main Module

The main module or UI Message Loop responsibility is to delegate tasks across the modules, by processing the information inputted by the user, received by the sensors and outputted through the vibration generator. Additionally, it also provides the UI which contains the controls and graphs with the acquired data so the user can observe the process in real time.

The UI enables the user to configure the acquisition and output settings, as well as control the execution of the acquisition process, among other features. All off this functionalities are triggered by interacting with buttons or inserting values in the appropriate fields.

The acquisition settings button triggers a separate window that provides three groups of settings, acquisition, trigger and logging, as shown in figure 31. The acquisition group enables the user to control the hardware and software parameters such as sample rate, input voltages and number of accelerometers. Additionally, it provides a low pass Butterworth Filter that may be enabled and set to a specific cutoff frequency at a given order.

Figure 31 – Data acquisition software UI with acquisition settings opened.

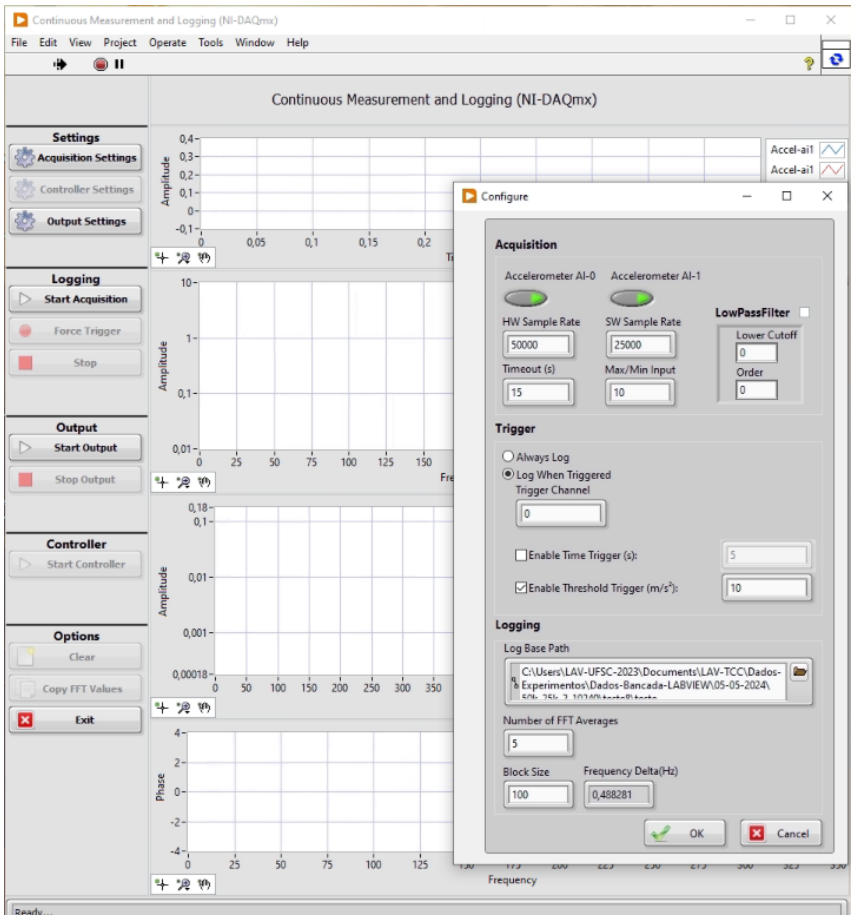

Source: Author (2024).

Figure 32 – Mandatory hardware setup variables abstracted from the end user.

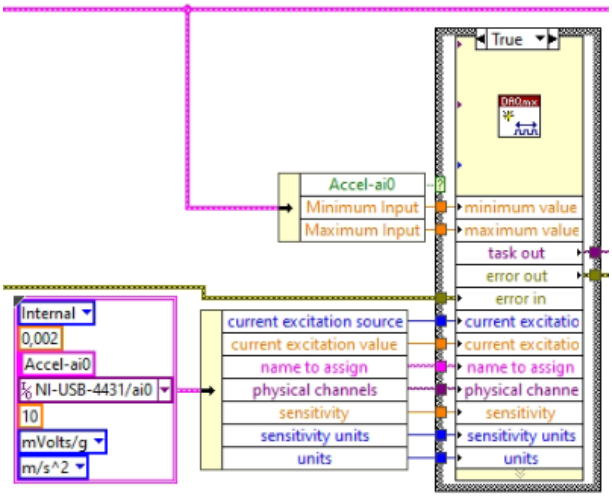

Source: Author (2024).

The trigger group provides settings for an automated start of the acquisition. The automation may be as function of the acceleration captured by the specified Trigger Channel or by a countdown timer. As for the logging group, it enables defining the system folder where the information acquired will be stored, as well as define number of averages and the block size for each FFT calculation.

Signal generation settings are contained in the output settings window. The generated signal may be stored and used repeatedly for consistency or generated for every execution of the signal output. During the development process it was observed that the host computer provided a signal with less noise than the signal generated by the output of the DAQ hardware due to the lack of a ground reference. Therefore, the final implementation of the vibration generator makes use of the audio output of the computer.

4.0.2 Data Acquisition Module

The process of acquiring data can be divided into three main stages: hardware setup, hardware initialization, and data acquisition. Each of these stages can be further broken down into smaller tasks, facilitating an efficient software implementation.

The hardware setup is responsible for declaring the mandatory variables for the hardware, it includes the hardware identification, hardware input variables, among several others shown in figure 32. Since the majority of this parameters persists across experiments, they were hard-coded into the application to simplify user interaction with the test bench. It should be noted that, if any hardware components are changed, these parameters should be checked against the components' data sheets to ensure an adequate setup.

Once all the required variables are defined, the LabVIEW application is able to interact with the specified hardware components. This interaction is achieved through the NI-DAQ™mx instrument driver, which provides tools for signal conditioning, hardware configuration and calibration, but most importantly for programming in LabVIEW at a high level of abstraction. Hardware initialization is achieved by defining the hardware inputs that shall enabled, defining a clock source and setting the DAQ hardware to a wait for the specified trigger to begin the acquisition.

The data acquisition process begins when the defined trigger is toggled and continues until the specified number of samples is collected. Each second, the DAQ hardware acquires the set number of samples based on the hardware sample rate. The data is then transferred to the computer at the defined software sample rate, which must be compatible with the data transmission capability of the USB interface.

4.0.3 Data Output Module

The data output process shares the same stages of the data acquisition module, although, one primary difference lies in the signal generation process, which must occur during the hardware initialization stage.

During the initial experiments, when generating signal through the NI-USB-4431, a frequency spike was observed close to 50 Hz which matched the output frequency of the Direct Current (DC) voltage source. Despite following the hardware setup guidelines and testing with multiple grounding configurations, therefore, the host computer sound output is used for the output signal generation.

Through the output settings dialog, the properties of the output signal can be defined (Figure 33). The software offers two types of signals: white noise and sine wave. It also allows for adjusting the output volume of the host computer's audio output and provides the option to trigger logging when the output is triggered. Additionally, the generated signal is stored for use in multiple experiments.

The sine wave requires the user to set only the frequency and magnitude of the signal. For the white noise, the signal is generated using a pseudo random number generator and consists of a uniformly distributed pseudo-random pattern within the signal amplifier's input voltage limits. Its spectral content can be reduced using a Low-Pass Filter (LPF) set to 350 Hz to fit the shaker's working range. Since the signal amplitude is reduced due to the LPF, a gain can be defined to restore the desired amplitude.

Figure 33 – User defined signal output settings.

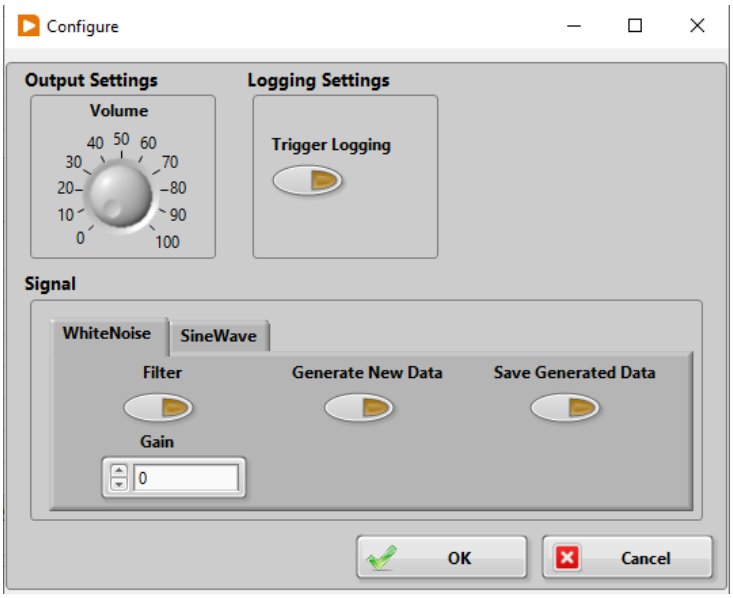

Source: Author (2024).

4.0.4 Data Logging Module

Once the initialization message is received, the module will initialize the text files that will store the session's logs, one for the raw data and a second one with the processed FFT values for each accelerometer. The module than waits for the trigger condition to be met to start writing the data.

In the data logging module, the process begins with applying a Hanning window to the time-domain acceleration signals to minimize spectral leakage. The data is then segmented into blocks of a specified size. For each block, the module computes the FFT, converting the time-domain signal into its frequency components. This produces a single-sided FFT spectrum that represents the RMS acceleration values. To enhance the spectral estimation, the module employs an averaging technique, averaging the current FFT spectrum with previously computed FFT spectra since the last reset of the averaging process. This averaging reduces random noise and provides a more stable and accurate representation of the signal's frequency content. Ultimately, the module returns both the magnitude and phase of the averaged spectrum.

5 RESULTS

The results obtained throughout the experiments are reported in this chapter. The first section presents the test bench's structure modal parameters obtained through EMA, followed by the statistical results that corroborate it's reliability. The subsequent sections present the acceleration magnitude curves resulting from the verification of the MPDs, with varying filling rates and different particle materials.

5.1 TEST BENCH VERIFICATION

The final test bench configurations with three and nine bushings were tested through EMA via impact testing. The resonance frequencies and respective damping values are displayed in Table 8.

Table 8 – Handlebar's modes obtained through EMA.

Mode	3 Bushings		9 Bushings	
	Frequency[Hz]	Damping[%]	Frequency[Hz]	Damping[%]
1	52.40	6.9	77.314	0.05
2	77.985	3.15	104.27	2.815
3	109.45	2.39	346.49	0.57
4	184.67	1.76		
5	286.078	1.12		
6				

Source: Author (2024).

When compared to the results obtained in previous studies, the values are concentrated within the expected range for a metallic handlebar. Although the studies have not reported the mass of the tested handlebars, it is plausible to assume that handlebars made of metal have similar thickness and diameter, and therefore exhibit comparable resonance frequencies.

The three-bushing setup exhibits rigid body modes at lower frequencies, for instance the one at 52.4 Hz. This proximity could potentially interfere with the handlebar's first vibration modes, particularly around 33 Hz. In contrast, the increased damping and rigidity of the nine-bushing configuration lead to a noisier FRF. This increased noise might be attributed to either insufficient excitation magnitude or inadequate duration of the excitation force relative to the recorded time domain duration.

5.2 MPD VERIFICATION

The following experiments were conceptualized based on the critical factors identified in the study of multiple particle dampers (MPDs). These experiments aimed to investigate if the effects of the material and filling rate could be monitored by the current setup.

After every trial the experiment results were observed so invalid test runs could be disposed immediately; thus, not influencing the acceleration magnitude averages. This process can be observed in figure 34 where the averages for five trials is lower than the average for the three highest meaning that some error occurred during acquisition and this trials should be removed from the overall average. Each block accounts for a separate run with the same test configuration.

Figure 34 – Standard plot for identifying acquired data discrepancies.

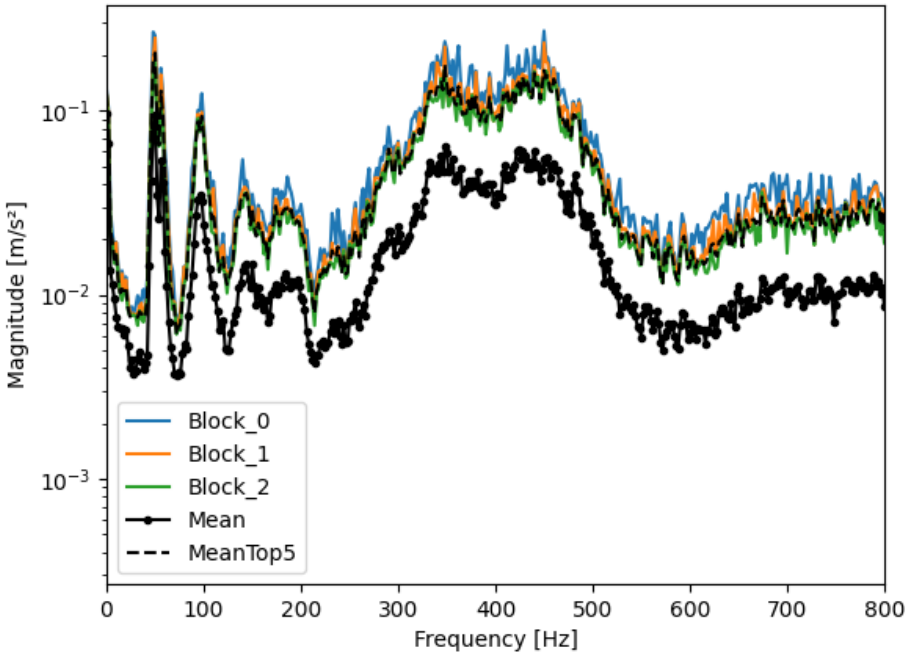

Once consistent data was acquired for all proposed test configurations. The batch processing algorithm was triggered to compile all the averages in the same plot. For the experiment where the filling rate was maintained in 90% (Figure 35) it is clear that the magnitude of the resonance was reduced and shifted to a lower frequency due to the mass increase.

From the data acquisition perspective, these results (Figure 35) highlight that a smaller frequency resolution would improve the comparison among the analyzed configurations. Additionally, even though the sample rate was set precisely at the Nyquist frequency, the absence of a low-pass filter for the input signal may have compromised the overall quality of the acquired data due to aliasing.

Figure 35 – Acceleration magnitude at the handlebar's extremity with a 90% filling rate.

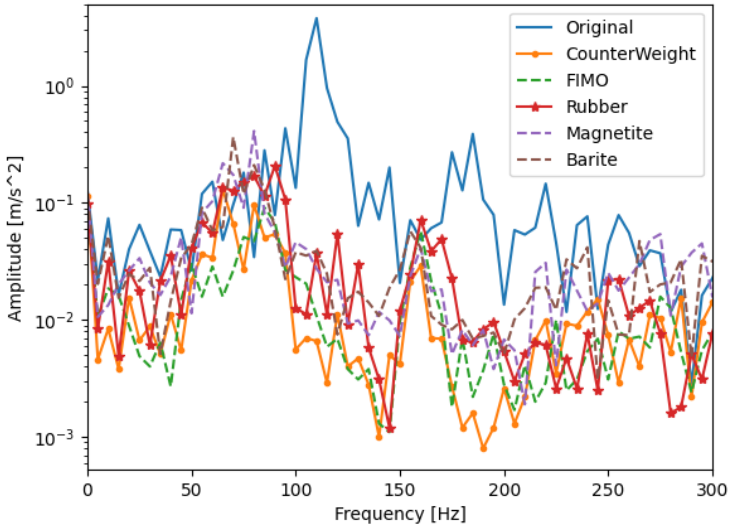

Source: Author (2024).

For the experiment with a fixed total mass, the influence of the filling rate is evident. The material with the highest filling rate, FIMO, yielded the best results among the tested materials (Figure 36). This observation aligns with Prasad et al. (2022), who concluded that a higher number of particles in the cavity increases contact and collision points, thereby enhancing the friction coefficient of the bulk material. Additionally, it can be observed that the FIMO-filled MPD, despite being 6.6% lighter than the counterweights, resulted in a similar magnitude.

Figure 36 – Comparison of different materials maintaining the same total mass.

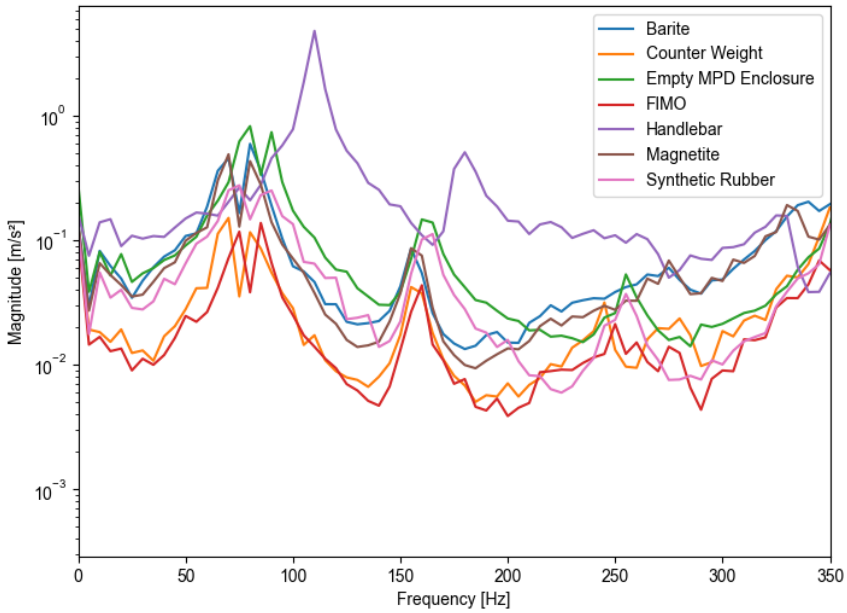

Source: Author(2024).

6 CONCLUSION

This work illustrates the differences among the currently used methods for verifying vibration absorbers and proposes a simple yet effective solution for comparing the efficiency of vibration absorbers. Both hardware and software enable the end user to excite the DUT with harmonic or random signals, maintaining consistency and reducing the complexity inherent in manual impact testing.

The experiments conducted with professional-grade equipment to gather test bench requirements involved a fully assembled handlebar. The appendices significantly influenced the measurements due to the stiffness of various materials composing the grips, hand-controls, and throttle. The throttle, in particular, not only has a surrounding grip but also some free play, which might disturb the measured values. Future experiments should consider exposing the metal of the handlebar by cutting through the grips to obtain more accurate measurements (Figure 17).

The EMAs conducted enabled comprehending aspects of the different test scenarios. The Free-Free method, where the DUT is suspended to simulate an unrestrained condition, is best suited for simplification of the dynamic response and resulted in the lowest signal to noise ratio when compared to the other fixture methods.

The foam-based fixture was intended to achieve a Free-Free condition; however, due to the geometry of the handlebar and the attached shaker, it couldn't be secured properly by the foam. This resulted in an unbalanced structure, introducing noise and complicating the process of distinguishing resonance frequencies. Additionally, it offers very low repeatability since each time the DUT is removed and placed back on the foam, it may experience different restraining forces.

The final design with rigid fixture presents similar challenges to the measurements conducted on the complete motorcycle, due to the test bench's structure complexity, which is a consequence of the high number of components and the resulting mass loading effects. Overall there is a compromise to made in order to enable testing with multiple appendices and using a controlled excitation source.

The selected shaker was able to provide the excitation necessary for reproducing both magnitude and frequency of the HAVs' spectrum. Although it does not contain embedded sensors to quantify the excitation input, the test bench fixture may be modified to provide an appropriate accelerometer mount or any other sensor that may be used for capturing the system's excitation input.

The final application meets the minimum requirements for verifying MPDs and provides a streamlined workflow, reducing the time spent on data acquisition and processing. The main limitation of the current setup is the lack of input monitoring which in turn limits the analysis that can be made without obtaining a FRF.

BIBLIOGRAPHY

ABU-MAHFOUZ, I. Data acquisition systems. *In*: ____. **Instrumentation: Theory and Practice, Part 1: Principles of Measurements**. Cham: Springer International Publishing, 2022. p. 115–138. ISBN 978-3-031-15246-7. Available from: https://doi.org/10.1007/978-3-031-15246-7_6.

AGOSTONI, S.; CHELI, F.; LEO, E.; PEZZOLA, M. An innovative multi dof tmd system for motorcycle handlebars designed to reduce structural vibrations and human exposure. **Mechanical Systems and Signal Processing**, v. 31, p. 298–315, 2012. ISSN 0888-3270. Available from: https://www.sciencedirect.com/science/article/pii/S0888327011005103.

ALLEMANG, R. J.; BROWN, D. L. Experimental modal analysis methods. *In*: ____. **Handbook of Experimental Structural Dynamics**. New York, NY: Springer New York, 2022. p. 533–613. ISBN 978-1-4614-4547-0. Available from: https://doi.org/10.1007/978-1-4614-4547-0_36.

ARUNACHALAM, M.; MONDAL, C.; SINGH, G.; KARMAKAR, S. Motorcycle riding posture: a review. **Measurement**, v. 134, p. 390–399, Oct. 2018.

ÅSTRÖM, C. et al. Hand-arm vibration syndrome (havs) and musculoskeletal symptoms in the neck and the upper limbs in professional drivers of terrain vehicles—a cross sectional study. **Applied Ergonomics**, v. 37, n. 6, p. 793–799, 2006. ISSN 0003-6870. Available from: https://www.sciencedirect.com/science/article/pii/S0003687005001572.

BERTOZZI, F. et al. Setup and method for assessing hand vibration and perceived discomfort during road race and gravel bike handlebars vibration. *In*: **2022 IEEE International Workshop on Sport, Technology and Research (STAR)**. [S.l.: s.n.], 2022. p. 89–93.

BRüEL & KJæR. **ACCELEROMETER SENSORS**. 2007. Available from: https://identidade.ufsc.br/versoes-do-brasao-para-fundos-claros/. Visited on: 16 fev. 2023.

CHELI, F.; PEZZOLA, M.; AGOSTONI, S. Objectification of the subjective riding comfort perception of motorcycles: Experimental analysis and international standards procedures. p. 928–933, 2011.

CHEN, H.-C.; CHEN, W.-C.; LIU, Y.-P.; CHEN, C.-Y.; PAN, Y.-T. Whole-body vibration exposure experienced by motorcycle riders – an evaluation according to iso 2631-1 and iso 2631-5 standards. **International Journal of Industrial Ergonomics**, v. 39, n. 5, p. 708–718, 2009. ISSN 0169-8141. Available from: https://www.sciencedirect.com/science/article/pii/S0169814109000754.

CHINDAMO, D.; GADOLA, M.; ARMELLIN, D.; MARCHESIN, F. Design of a road simulator for motorcycle applications. **Applied Sciences**, v. 7, p. 1220, 11 2017.

COSSALTER, V. **Motorcycle Dynamics**. 2. ed. Morrisville: Lulu, 2006.

DIYANA, M. et al. Risk factors analysis: work-related musculoskeletal disorders among male traffic policemen using high-powered motorcycles. **International Journal of Industrial Ergonomics**, v. 74, n. 102884, Nov. 2019.

EHLERS, T.; LACHMAYER, R. Design of a motorcycle triple clamp optimised for stiffness and damping. *In*: THE MUNICH SYMPOSIUM ON LIGHTWEIGHT DESIGN 2020, 1., Munich. **Proceedings...** Berlin, Heidelberg: Springer Berlin Heidelberg, 2020. p. 1–17.

EHLERS, T.; TATZKO, S.; WALLASCHEK, J.; LACHMAYER, R. Design of particle dampers for additive manufacturing. **Additive Manufacturing**, v. 38, p. 101752, 2020. ISSN 2214-8604. Available from: https://www.sciencedirect.com/science/article/pii/S2214860420311246.

EUROPEAN PARLIAMENT. **Directive 2002/44/EC - Vibrations**. [S.l.], 2002. Available from: https://eur-lex.europa.eu/legal-content/EN/TXT/HTML/?uri=CELEX:32002L0044. Visited on: 10 Oct. 2023.

FALCO, D. de; MASSA, G.; PAGANO, S.; STRANO, S. Motorcycle handlebar dynamic response: Theoretical and experimental investigation. **International Review of Mechanical Engineering**, v. 7, p. 795–801, 01 2013.

FASANA, A.; GIORCELLI, E. A vibration absorber for motorcycle handles. **Meccanica**, v. 45, n. 1, p. 79–88, 2010. Available from: https://doi.org/10.1007/s11012-009-9229-8.

GATTI, P. L. **Applied Structural and Mechanical Vibrations: Theory, Methods and Measuring Instrumentation**. London: CRC Press, 1999. Available from: https://api.semanticscholar.org/CorpusID:29581650.

GRIFFIN, M. **13 - An Introduction to Hand-transmitted Vibration**. London: [s.n.], 1990. 531-551 p. ISBN 978-0-12-303040-5. Available from: https://www.sciencedirect.com/science/article/pii/B9780123030405500179.

HANLY, S. **Why the Power Spectral Density (PSD) Is the Gold Standard of Vibration Analysis**. 2020. Available from: https://blog.endaq.com/why-the-power-spectral-density-psd-is-the-gold-standard-of-vibration-analysis. Visited on: June 10, 2023.

INMAN, D. **Engineering Vibration**. New Jersey: Pearson, 2014. ISBN 978-0-13-287169-3.

ISO. **Mechanical vibration - Measurement and evaluation of human exposure to hand-transmitted vibration - Part 1: General requirements**. Geneva, Switzerland, 2001.

ISO. **Mechanical vibration - Measurement and evaluation of human exposure to hand-transmitted vibration - Part 2: Practical guidance for measurement at the workplace**. Geneva, Switzerland, 2001.

JELACIC, Z.; PIKULA, B. Vibration analysis of motorcycle handles. **Lecture Notes in Networks and Systems**, p. 196–201, 01 2019.

KHUNE, S.; BHENDE, A. Vibration analysis of motorcycle handlebar for riding comfort using tuned mass damper. **Journal of Measurements in Engineering**, v. 8, 12 2020.

LU, Z.; LIAO, Y.; HUANG, Z. Stochastic response control of particle dampers under random seismic excitation. **Journal of Sound and Vibration**, v. 481, p. 115439, 2020. ISSN 0022-460X. Available from: https://www.sciencedirect.com/science/article/pii/S0022460X20302716.

LU, Z.; WANG, Z.; MASRI, S. F.; LU, X. Particle impact dampers: Past, present, and future. **Structural Control and Health Monitoring**, v. 25, n. 1, p. e2058, 2018.

MEYER, N.; SEIFRIED, R. Toward a design methodology for particle dampers by analyzing their energy dissipation. **Computational Particle Mechanics**, v. 8, p. 681 – 699, 2020. Available from: https://api.semanticscholar.org/CorpusID:229051535.

MIRBOD, S. M. et al. Assessment of hand-arm vibration exposure among traffic police motorcyclists. **International Archives of Occupational and Environmental Health**, v. 70, n. 1, p. 22–28, Nov. 1997.

NOH, J.; MD REZALI, K. A.; AS'ARRY, A.; JALIL, N. Transmission of vibration from motorcycle handlebar to the hand. **Journal of the Society of Automotive Engineers Malaysia**, v. 1, p. 191–197, 09 2017.

OSPINA, H.; JIMÉNEZ, L. Understanding the impact of physical fatigue and postural comfort experienced during motorcycling: a systematic review. **Journal of Transport & Health**, v. 12, p. 290–318, Mar. 2019.

PODOSEK, K.; SARIC, Z.; ZUSKA, A. Test bench for the assessment of vibrations occurring in motorcycles. **The Archives of Automotive Engineering/ Archiwum Motoryzacji**, v. 95, p. 65–78, 03 2022.

PRASAD, B. B.; DUVIGNEAU, F.; JUHRE, D.; WOSCHKE, E. Damping performance of particle dampers with different granular materials and their mixtures. **Applied Acoustics**, v. 200, p. 109059, 2022. ISSN 0003-682X. Available from: https://www.sciencedirect.com/science/article/pii/S0003682X22004339.

RAJPER, S. Z.; ALBRECHT, J. Prospects of electric vehicles in the developing countries: a literature review. **Sustainability**, v. 12, n. 5, p. 1906, Mar. 2020.

RANDALL, R. B.; ANTONI, J.; BORGHESANI, P. Applied digital signal processing. *In*: ____. **Handbook of Experimental Structural Dynamics**. New York, NY: Springer New York, 2020. p. 1–81. ISBN 978-1-4939-6503-8. Available from: https://doi.org/10.1007/978-1-4939-6503-8_6-1.

RASHID, H.; OMAR, A.; MAHMUD, Z.; FAUZI, W. Musculoskeletal disorders (msds) among non-occupational motorcyclists: What are the issues? **Asian Journal of University Education**, v. 16, p. 220, 01 2021.

RICHIEDEI, D.; TAMELLIN, I.; TREVISANI, A. Beyond the tuned mass damper: a comparative study of passive approaches to vibration absorption through antiresonance assignment. **Archives of Computational Methods in Engineering**, v. 29, n. 1, p. 519–544, 2022. Available from: https://doi.org/10.1007/s11831-021-09583-w.

RO, J.-J.; CHIEN, C.-C.; WEI, T.-Y.; SUN, S.-J. Flexural vibration control of the circular handlebars of a bicycle by using mfc actuators. **Journal of Vibration and Control**, v. 13, p. 969 – 987, 2007. Available from: https://api.semanticscholar.org/CorpusID:122791014.

SCHALDENBRAND, P. **Human Body Vibration**. 2021. Available from: https://community.sw.siemens.com/s/article/Human-Body-Vibrationhttps://community.sw.siemens.com/s/article/Human-Body-Vibration.

SETIA, S.; KUWAR, V.; PAWAR, P. R.; JAMBHALE, M. S.; SARAF, M. R. Active control using smart materials for 2-wheeler handle bar vibration. *In*: **2019 IEEE Transportation Electrification Conference (ITEC-India)**. [S.l.: s.n.], 2019. p. 1–5.

SáNCHEZ, M.; ROSENTHAL, G.; PUGNALONI, L. A. Universal response of optimal granular damping devices. **Journal of Sound and Vibration**, v. 331, n. 20, p. 4389–4394, 2012. ISSN 0022-460X. Available from: https://www.sciencedirect.com/science/article/pii/S0022460X12003513.

USAMAH, N.; AHMAD MAZLAN, A. Z.; RIPIN, Z. mohd. Investigation of motorcycle handle vibration attenuation using a suspended handlebar with different rubber mount characteristics. **International Journal of Acoustics and Vibrations**, v. 27, p. 276–284, 09 2022.

WANG, Q.; DAN, D. A simplified modeling method for multi-particle damper: Validation and application in energy dissipation analysis. **Journal of Sound and Vibration**, v. 517, p. 116528, 2022. ISSN 0022-460X. Available from: https://www.sciencedirect.com/science/article/pii/S0022460X21005563.

YANG, F.; SEDAGHATI, R.; ESMAILZADEH, E. Vibration suppression of structures using tuned mass damper technology: A state-of-the-art review. **Journal of Vibration and Control**, v. 28, n. 7-8, p. 812–836, 2022. Available from: https://doi.org/10.1177/1077546320984305.

YOKOMORI, M.; NAKAGAWA, T.; MATSUMOTO, T. Handlebar vibration of a motorcycle during operation on different road surfaces. **Scandinavian Journal of Work, Environment & Health**, n. 4, p. 332–337, Aug 1986. ISSN 0355-3140.

YOUSIF, M. T.; SADULLAH, A. F. M.; KASSIM, K. A. A. A review of behavioural issues contribution to motorcycle safety. **IATSS Research**, v. 44, n. 2, p. 142–154, 2020. ISSN 0386-1112. Available from: https://www.sciencedirect.com/science/article/pii/S038611121930072X.